HSL, Harpur Hill
Buxton, SK17 9JN
Tel. 01298 218000
Fax. 01298 218590

HEALTH & SAFETY LABORATORY

Post Hatfield Rolling Contact Fatigue

Measurement of Crack Depths in a Section of Head Hardened Rail

MM/04/05

Project Leader: **Dr J W Hobbs**
Author(s): **J T Dutton, BSc, J W Hobbs, PhD, D I Fletcher*, PhD, A Kapoor*, PhD**
Science Group: **Engineering Control**
***University of Newcastle**

OFFICE OF RAIL REGULATION

DISTRIBUTION

Dr D Hoddinott (3)	RI TD Authorising Officer
Dr N G West	HSL Operations Director
Mr P F Heyes	Engineering Control Group, HSL
Prof J Beynon	University of Sheffield
Dr M Frolish	University of Sheffield
Prof A Kapoor	University of Newcastle
Dr D Fletcher	University of Newcastle
Dr J W Hobbs	HSL
Group Circulation (4)	HSL
Section File	
Registry File	
LIS (2)	

PRIVACY MARKING:

Not to be communicated outside HSE without the approval of the Authorising Officer.

HSL report approval:	Dr W Geary
Date of issue:	March 2005
Job number:	JR31086
Registry file:	MM/PR/21
Electronic filename:	H:\Work\HSE\Research\JR31086 - RCF\crack_morphology.doc

CONTENTS

EXECUTIVE SUMMARY

The current report is part of an ongoing investigation into the phenomenon of rolling contact fatigue in rails. HSE is funding a two-year programme, which focuses on:

[1] A three dimensional assessment of the crack morphology observed in head hardened rail.
[2] The cause of crack branching (using whole-life model).
[3] The role of residual stress in the development of rolling contact fatigue cracks.
[4] The influence of pro-eutectoid ferrite and decarburisation on crack growth.

Presented here is the work carried out to measure the cracks present in a 304 mm long length of head hardened rail.

The grinding of the rail section revealed a large number of cracks of various depths. Analysis of the data obtained from this exercise has enabled the following conclusions to be drawn:

1. Cracks grow at shallow angles, generally between 0° and 15°, until they reach a depth of approximately 6 mm.

2. The angle of cracks is particularly shallow between depths of 1.5 mm and 3 mm, with average angles of less than 1.5°.

3. The cracks tend to turn down into the rail head steeply at depths of over 6 mm. The majority of crack segments with depths above 7 mm have angles of over 30°.

4. Of the sample of cracks that were analysed for the relationship between surface length and depth, four lay outside the region expected by the Railtrack model. Therefore, these cracks were deeper than the Railtrack model predicted, based on the measured surface length of the cracks.

5. A three-dimensional model has been generated to help to visualise the cracks in the rail head.

1 INTRODUCTION

In order to investigate the phenomenon of rolling contact fatigue in rails, HSE is currently sponsoring work specifically on head hardened rail, focusing on:

[1] A three dimensional assessment of the crack morphology observed in head hardened rail.
[2] The cause of crack branching (using whole-life model).
[3] The role of residual stress in the development of rolling contact fatigue cracks.
[4] The influence of pro-eutectoid ferrite and decarburisation on crack growth.

This report details the experimental work carried out on a section of head hardened rail to measure the cracks present in the rail. The data produced has been incorporated in a three dimensional model representing the cracks observed in the rail section by the University of Sheffield which is included in this report as Appendix 1.

By examining the morphology of the crack in a section of rail, a better understanding of the way cracks propagate through rails is possible. Of particular interest is the conditions under which small, shallow cracks turn down into the rail head.

2 EXPERIMENTAL

2.1 GRINDING OF RAIL

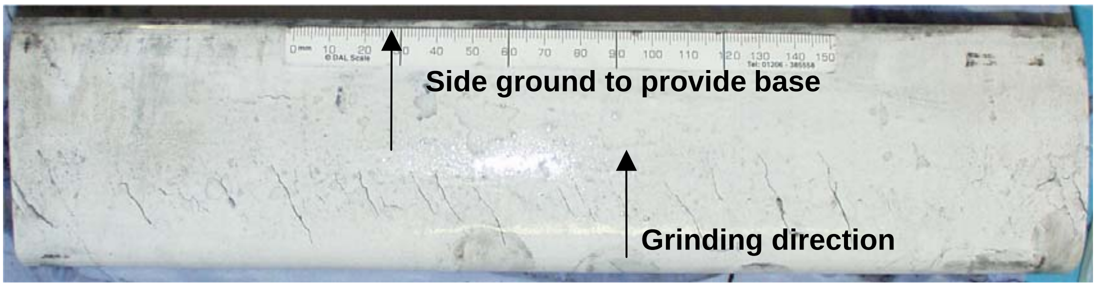

Figure 1 Top view of head hardened rail prior to grinding

A section of head hardened rail approximately 304 mm in length, identified as H2-H710 was identified for use in the project. The width of the rail was approximately 70.7 mm. The head section of the rail was detached from the web and foot. The section was sprayed with white contrast paint and then non-destructively tested using a magnetic particle technique to highlight any cracks present in the crown of the rail, as shown in Figure 1. The contrast paint was used to aid the detection of defects, as any defects would show as fine black lines on the white contrast background. It was decided that the section exhibited sufficient numbers of cracks to provide useful data for this investigation.

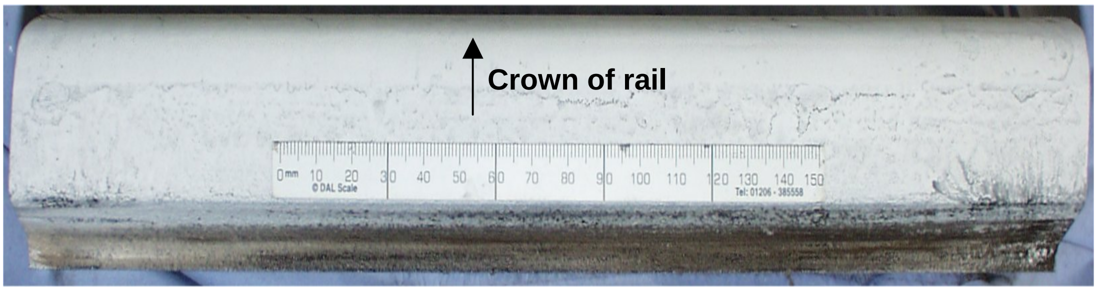

Figure 2 Side view of head hardened rail prior to grinding

The rail section was then ground on the field side to provide a flat and stable base to allow grinding to take place on the gauge side. Before grinding commenced, the gauge side was sprayed with contrast paint and then magnetic particle inspected. The gauge side was then photographed using a digital camera to record its initial condition, as shown in Figure 2. Grinding was undertaken using a flat bed surface grinder. Approximately 1 mm of material on the gauge corner side was removed from the length and width of the rail head. Once the material had been removed the ground surface was cleaned and white contrast paint applied. If any defects were present the whole of the section was photographed using four separate images, which overlapped to ensure that the whole length of the rail section was recorded. Two rulers were placed on the ground surface below the defects, to give scale to the photographs, as shown in Figure 3. Digital images were stored to allow analysis to take place once the grinding program had been completed.

The process of grinding and inspection was repeated. The first defects were detected on the 9th grinding increment, when approximately 7.2 mm of material had been removed. The grinding process continued for a total of 44 increments, until no further defects could be observed along the length of the section. A total of approximately 47.8 mm of material was removed.

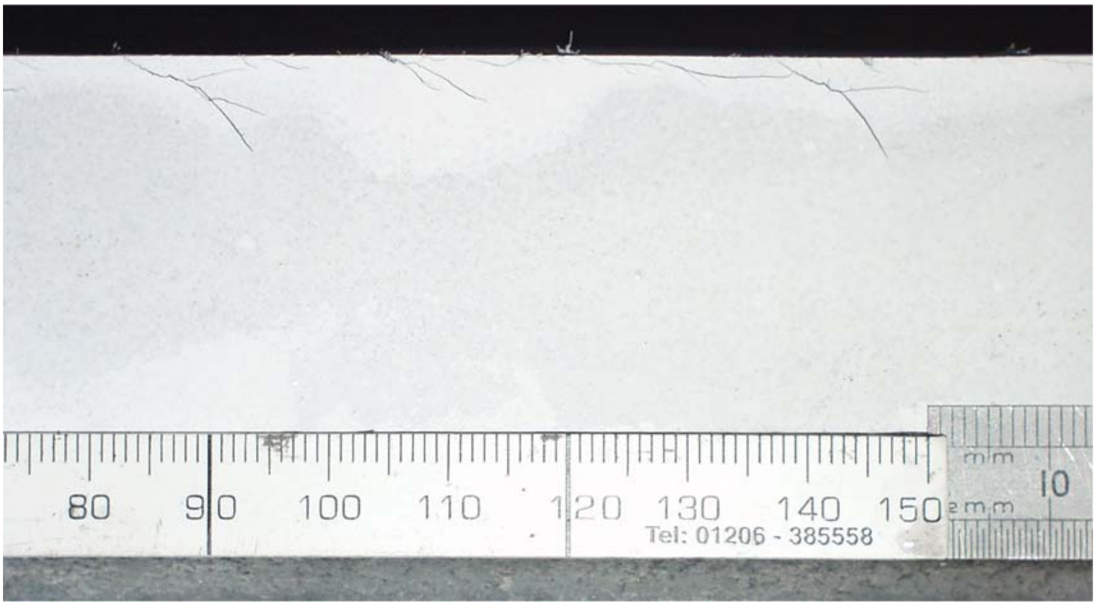

Figure 3 Example of defects and scale

3 ANALYSIS

3.1 RECORDING DATA

To produce data that could be incorporated in a digital model, the distance of the defect along the length and depth of the rail head was required. A software programme called Optimas was acquired, into which digital images of the defects could be imported and this allowed measurement of the X and Y coordinates of each defect. By calibrating the software using the ruler scales present in each image, it was possible to output data in millimetres, accurate to approximately ±0.2 mm. The four images from each increment, were individually analysed and the defect data stored in a file. These data files were then loaded into an Excel spreadsheet where they were merged to produce a single data set, which contained the X and Y coordinates measurements for each defect.

3.2 VISUALISATION MODEL

The University of Sheffield processed the data obtained to generate a model in which the cracks could be observed from any angle and rotated. Full details of the generation of the model and examples of the output can be found in Appendix 1.

3.3 CRACK ANALYSIS

To investigate the correlation between visible surface crack length and crack depth, the measured characteristics were defined as shown in Figure 4. Straight lines were used to measure distances, rather than following the intricate path of each crack. Due to time constraints, only a selection of cracks were measured in this way, the 22 deepest cracks being chosen. More details regarding the analysis method can be found in Appendix 1.

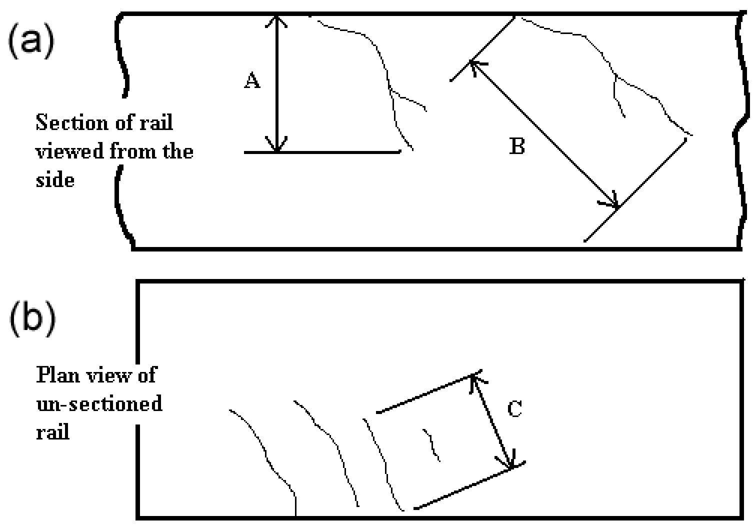

Figure 4 Definitions of crack measurement. (a) A section view of the rail. Crack A is deeper than crack B, although crack B is longer, hence different groups of cracks were identified when searching for the longest and deepest sets. (b) Plan view of the rail prior to sectioning, illustrating visible crack lengths

A statistical analysis of the data was performed in an attempt to quantify the likely angle of cracks for given depths. Figure 5 shows a schematic diagram of a typical crack with the data points marking out the shape of the crack. The length of a segment is also shown. The angle of each segment, from one data point to the next, was calculated, and defined as positive growing into the rail in the same direction as the traffic, as shown in Figure 5. Positive angles greater than 90° were therefore defined as growing against the traffic and negative angles were defined as growing up towards the rail surface.

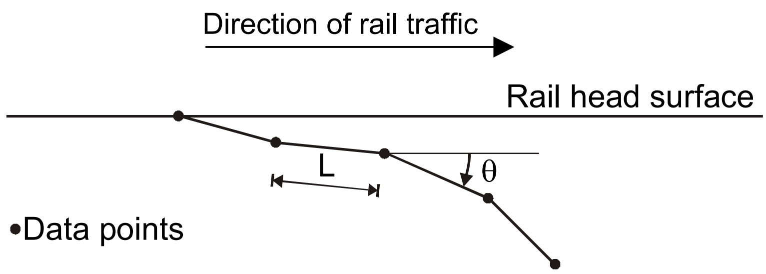

Figure 5 Schematic diagram of crack showing length of segment (L) and angle (θ)

The next stage was to determine the degree to which the crack changed angles as it grew, effectively trying to quantify the smoothness of crack. To do this, the difference in crack angles was calculated between neighbouring segments, by subtracting the angle of the previous segment, i.e. $\theta_2 - \theta_1$ as shown if Figure 6.

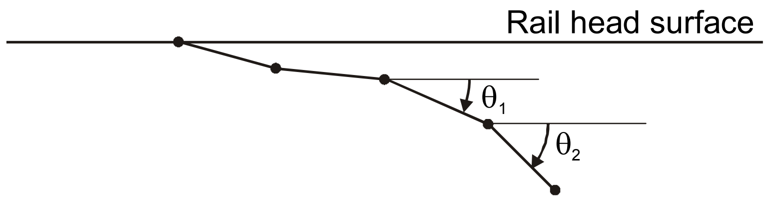

Figure 6 Calculation of change in angle between adjacent segments ($\theta_2 - \theta_1$)

The mean crack angle was calculated by averaging the crack angles over different ranges of crack depths. The cracks were deemed to lie at the depth of the first data point, as shown in Figure 7. The depth ranges over which angles were averaged had an interval of 0.5 mm.

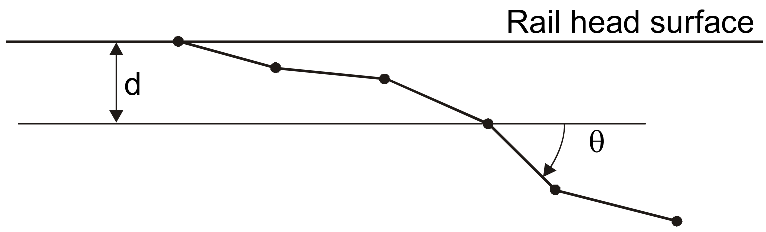

Figure 7 Depth of crack for single segment angles

In addition to averaging the crack angles for the different depth ranges, the distribution of angles was plotted. Intervals of 15° were used for the crack angles. Two distributions were generated; the first for the angles of a single segment and the second for the angles obtained over two segments, as shown in Figure 8. In the case of the two-segment angles, the corresponding depth was taken as the depth of the middle data point.

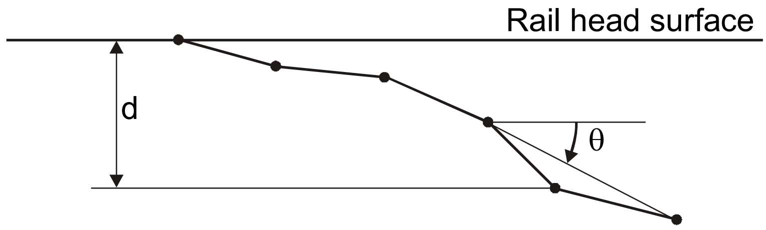

Figure 8 Depth of crack for double segment angles

4 RESULTS AND DISCUSSION

4.1 DATA CHARACTERISATION

4.1.1 Segment length and Angle Variation

Figure 9 shows the distribution of the segment lengths, with an interval of 0.1 mm. As can be seen, the mode length is in the range 0.6 to 0.7 mm, labelled as the midpoint length, 0.65 mm. Although there is a wide range of segment lengths, with some segments over 2 mm in length, 56% of segments are within the range 0.4 mm to 0.8 mm.

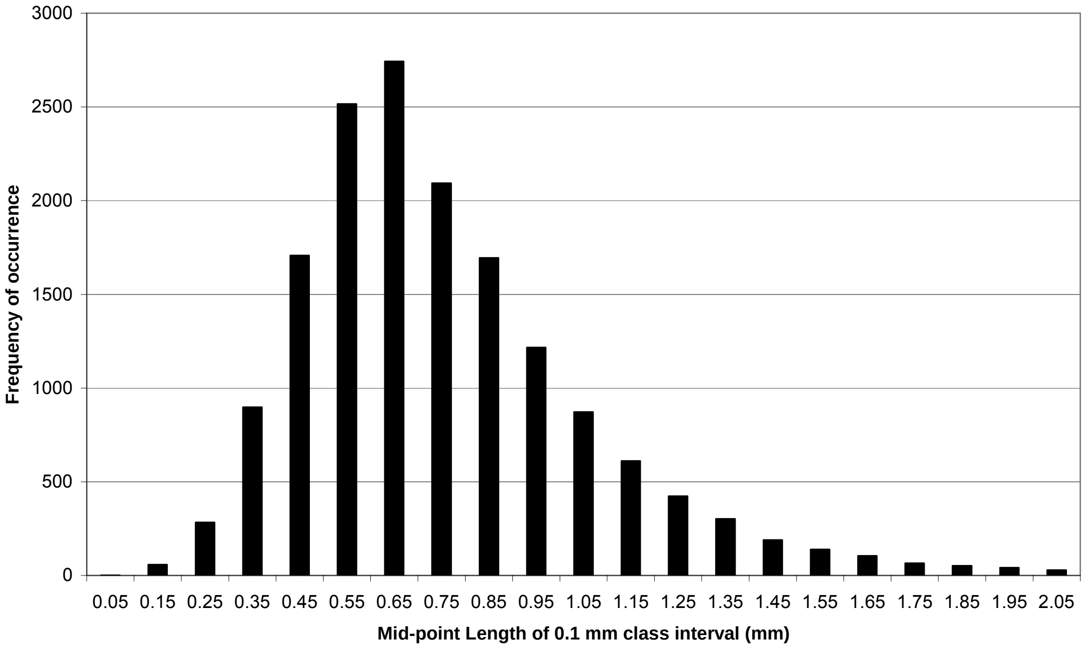

Figure 9 Distribution of segment lengths

The variation in angle between one segment and the next is shown in Figure 10. A positive angle represents a crack that is becoming steeper down into the rail head. The range 0 to 5 degrees change is by far the most common change. This is in part due to the fact that this range includes the zero degree changes, which are more common due to rounding. A number of points that would have had small negative angles have been rounded to zero, increasing the count in the $0 \leq \theta < 5$ range at the expense of the $-5 \leq \theta < 0$ range.

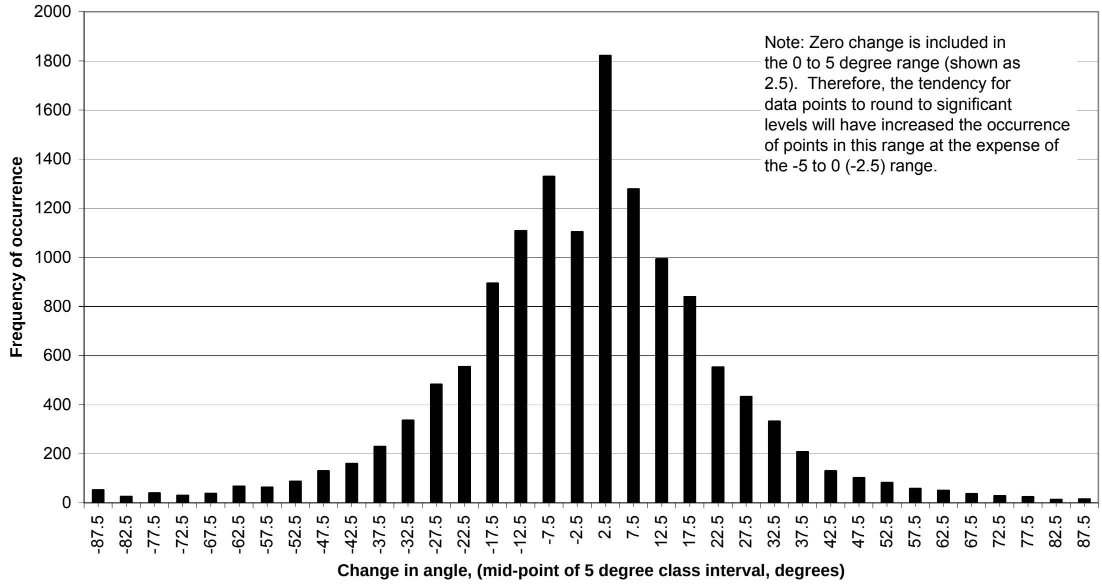

Figure 10 Change in angle between adjacent segments

The same data is shown in cumulative form in Figure 11. For example, in 54% of cases, the angle a segment will lie within ±15° of the previous segment, and 80% lie within ±30°. This indicates that the cracks are relatively smooth, without excessive angle changes. Sudden changes of angle were rare. This may, at least partly, be due to sampling effects, where more data points would be used in areas of significant angle change, effectively splitting large angles into a number of smaller angular changes.

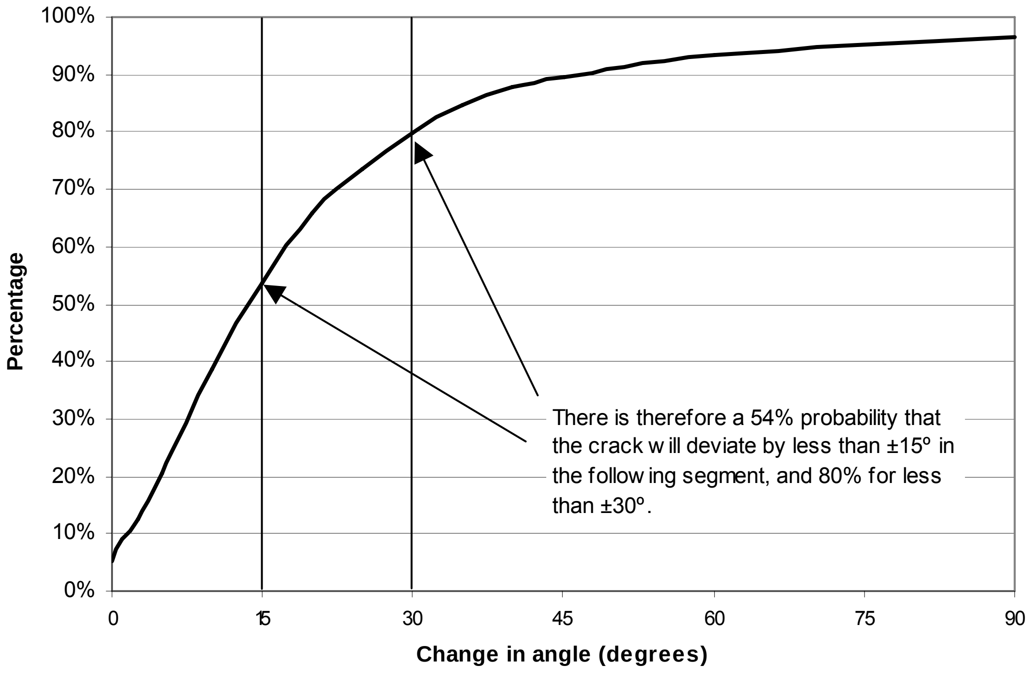

Figure 11 Cumulative change in angle between adjacent segments

4.2 SURFACE LENGTH / DEPTH CORRELATION

The distribution of crack depths against visible surface crack length is shown in Figure 12 for the 22 cracks analysed in this way. The points are shown superimposed on to a diagram used by Railtrack to estimate the likely depth of cracks [1], where cracks can be of any depth within the shaded region. The Railtrack relationship between surface length and depth implies that for a crack with a surface length of less than 20 mm, the depth of the crack is not expected to exceed 5 mm.

It can be seen that there is a general agreement between the current results and the Railtrack literature. This indicates that the crack growth pattern in the rail sample is consistent with the results previously obtained by Railtrack. However, four points do lie outside the shaded region, with a further four points lying close to the border of the shaded region. Three of the points lying outside have a surface length significantly below 20 mm, although they exceed the 5 mm depth by a small amount. The fourth point outside the shaded region has a surface length of almost 20 mm, but the depth far exceeds 5 mm. It is clear that the Railtrack model may be non-conservative. It should be noted that as only the deepest cracks were analysed there would be many more cracks lying within the shaded regions if all the cracks had been used. Further detail can be found in Appendix 1.

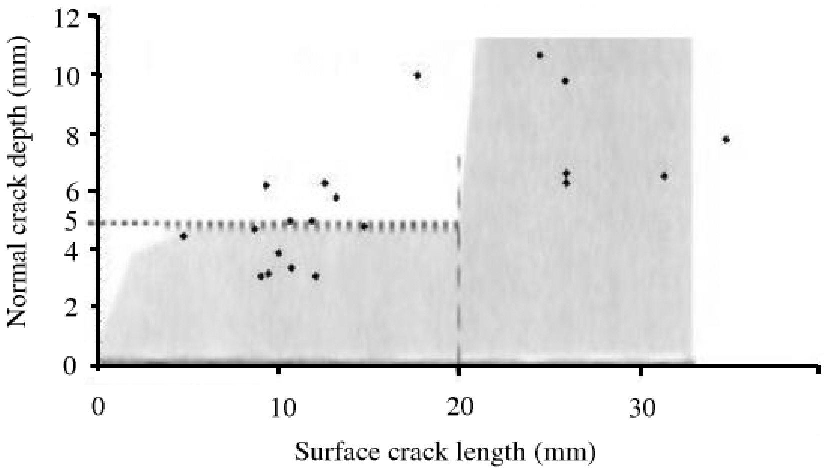

Figure 12 Combined plot of normal crack depth and surface crack length obtained from Railtrack and rail section

4.3 CRACK DEPTH AND ANGLE

Figure 13 shows all the data points generated by calculating the angle of the crack segments plotted against the depth of the first point of each segment. A number of points can be noted from this chart. Firstly, it is clear that there are too many points on the chart to be able to distinguish all the individual points. The area between 0 and 5 mm in depth with an angle of between –30° and 45° in particularly densely populated with points. It should be remembered that data points at shallow depths will predominate since data points are generated all the way along the crack. Therefore, long, deep cracks will have points at shallow depths, not just at the crack tip.

It is clear that a certain degree of rounding has occurred, with points converging around 0°, 45° and 90°. Given that the system for marking the data points on the original photographs of the ground sections had a certain resolution, this is not surprising.

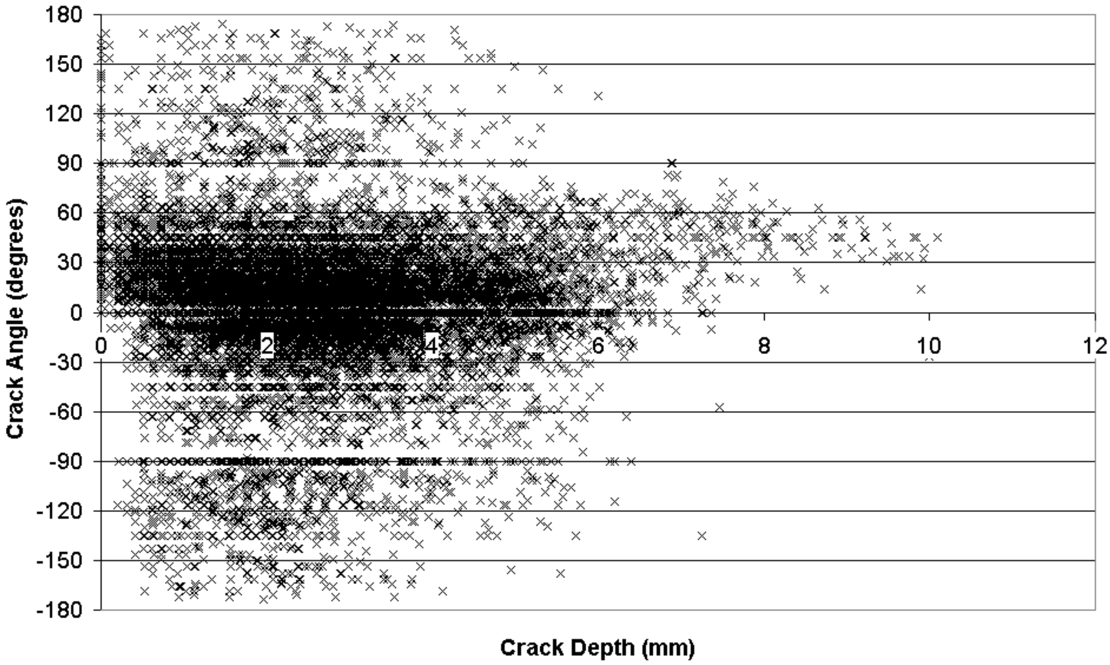

Figure 13 Distribution of crack angles with depth

Figure 14 shows the number of data points lying at different depths below the rail surface. The depth range containing the highest number of data points is between 1.5 and 2.0 mm, with the wider range of 1mm to 3 mm containing many points. This suggests that the cracks were growing through this range at a shallower angle than at shorter depths. The relative scarcity of points at larger crack depths is likely to be due to the smaller number of deep cracks, and therefore does not necessarily give any statistically valid information about the crack angles in this area.

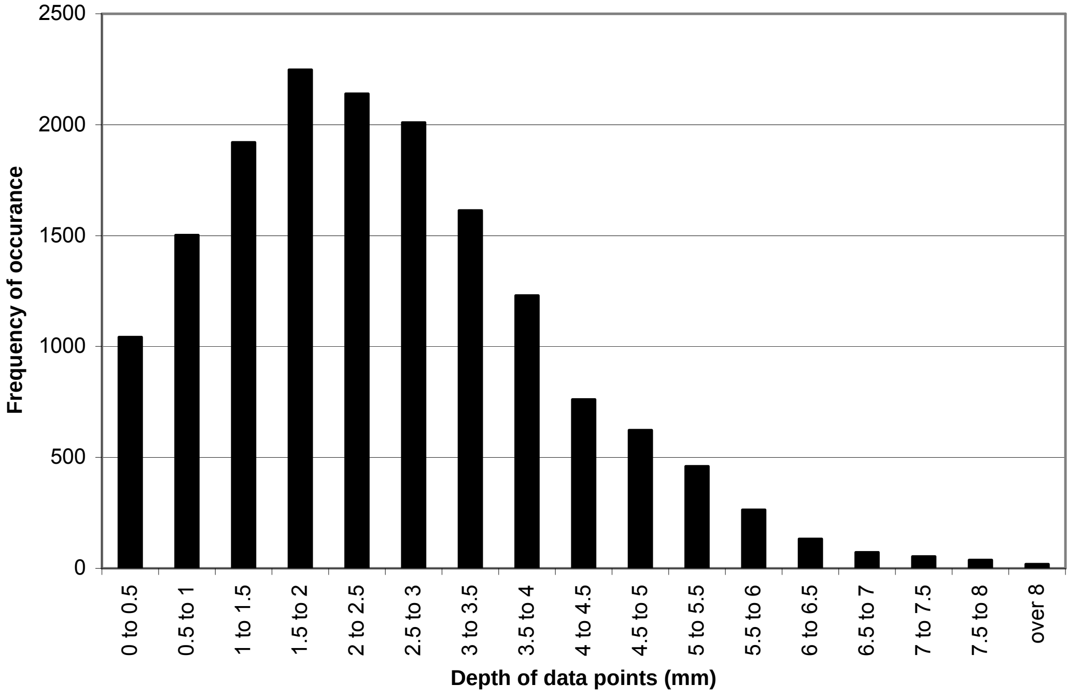

Figure 14 Number of data points against depth

The average angles of the cracks, calculated for 0.5 mm depth ranges, are shown in Figure 15. As the depth of each segment is taken as the first data point of the segment it is not possible for a crack at zero depth to have a negative angle. The absence of any negative angles at 0 mm depth explains the higher positive value for the mean crack angle for the range 0 mm to 0.5 mm (shown at the mid-point of the interval, i.e. 0.25 mm). Between a depth of 1.5 mm and 3 mm, the mean angle is very low, although still positive, indicating that in general the cracks grow almost parallel to the rail surface. This is supported by Figure 14, which shows the highest number of data points within this region.

As the crack depth increases beyond 6.5 mm, the mean angle increases quickly to average approximately 40° above this depth.

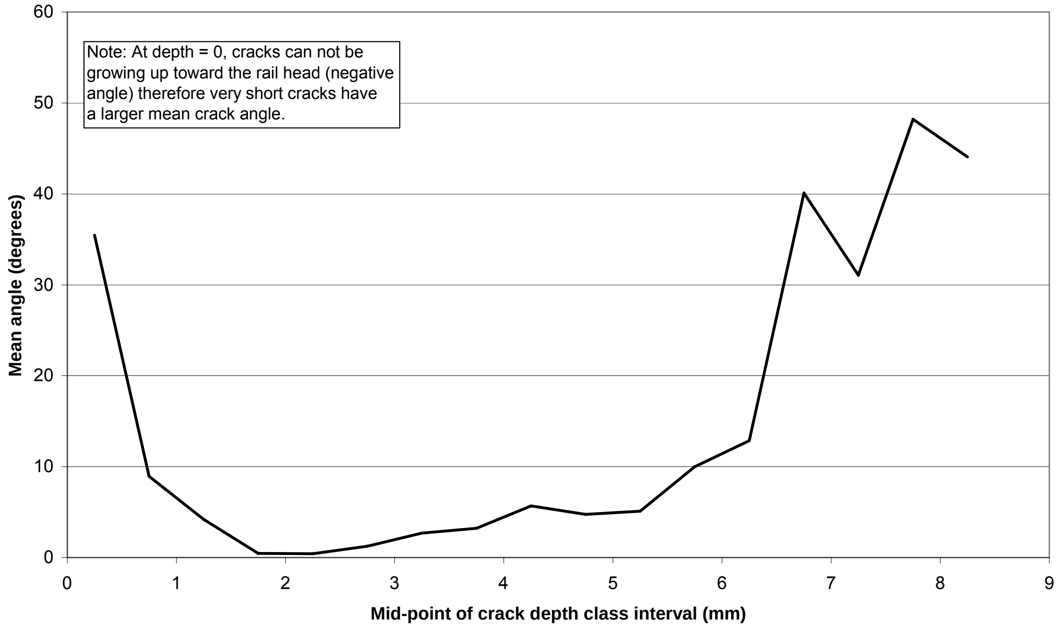

Figure 15 Average crack angle against depth

A more detailed breakdown of the distributions of the crack angles with depth is shown in Figure 16 and Figure 17. These figures show how the ranges of angles are distributed for each 2 mm range interval of depth when calculating the crack angle over one or two segments respectively. The angles are grouped into 15° intervals.

The angles for the 0 to 2 mm depth range show a broad distribution, with almost equal numbers occurring between 0 to 45 degrees. As the depth increases, the distribution of angles narrows, centring on the 0 to 15° range. For the ranges covering 2 mm to 6 mm depth, 35% of angles are within this range. Above 6 mm, a second peak starts to appear for the 30° to 45° range. This range increases at the expense of the 0 to 15° range until over 50% of segments have angles in the 30° to 45° range for crack depths of over 8 mm.

Averaging the angles over two segments does not significantly change the distribution described above. This gives confidence that the distribution observed is not a function of the sampling rate of the data.

However, it should be noted that the number of data points at depths over 7 mm is low, and represents only a few separate cracks and therefore the data obtained may not be representative.

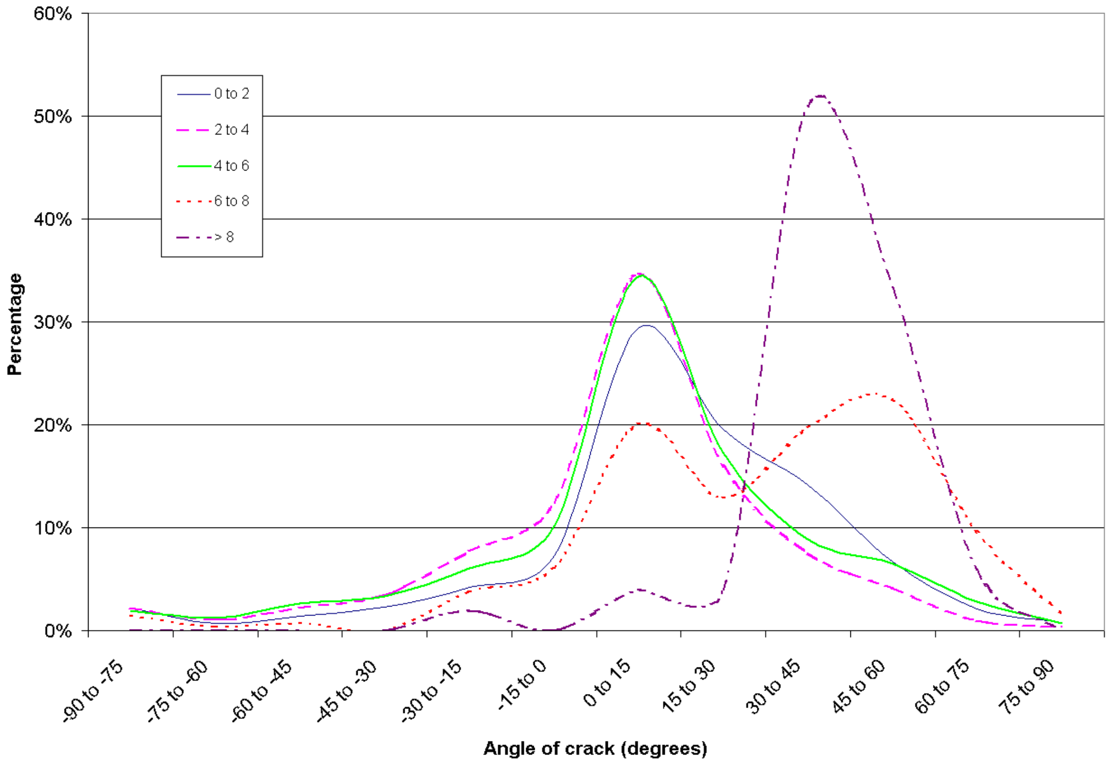

Figure 16 Distribution of crack angles of single segments at different depths

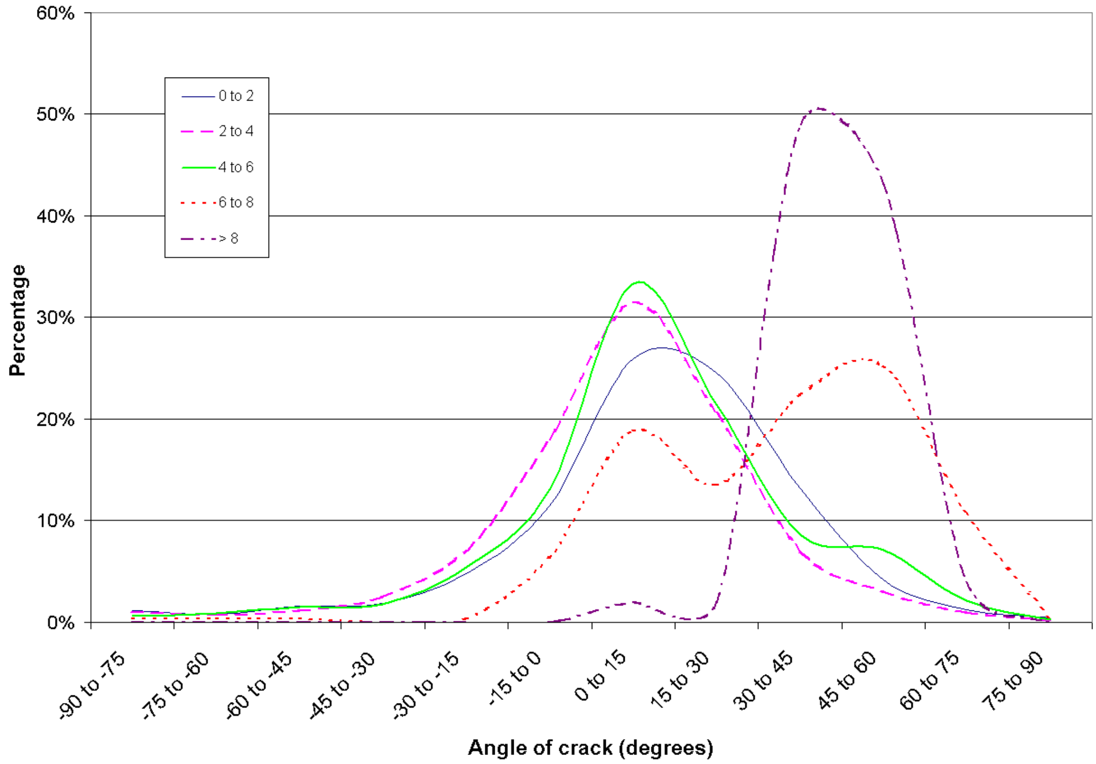

Figure 17 Distribution of crack angles of double segments at different depths

4.4 THREE-DIMENSIONAL ANALYSIS

All the above analysis considers just the crack angles in the plane of the section.

To obtain more information from the crack data it was decided to calculate the angles of crack growth at various depths in the rail. Initially these angles were determined by connecting adjacent points within the data. However, scatter within the measurements produced large variability in the angles, and there was some dependence of the angles on the separation of the data points.

Progressing from a two-dimensional view of the cracks (i.e. crack paths on a single plane through the rail) to a full three-dimensional view of the cracks exacerbated the problems of connecting adjacent points in the data. To overcome these problems it was decided to use Matlab to find a "best-fit" surface through the data points allowing smoothing of the three-dimensional data, thereby revealing the underlying angle and form of the cracks. The angle of each "facet" of this fitted surface could then be found to summarise the change of crack orientation with position inside the rail head.

4.4.1 Method

Using Matlab a surface is fitted to data representing points on the crack surface. The dataset must therefore contain points from the surface of only one crack, and pre-processing of raw data is required to separate out points from a single crack.

The surface to be fitted to the crack data is defined by a grid of points which is regularly spaced in the plan view, i.e. when viewed from above the rail. The density of this grid determines the smoothing applied to the original data. If the grid is of similar density to the original data points little smoothing will be applied. A grid that is too coarse will not allow the significant features of the crack to be represented in the output. Finding the optimum grid size must be carried out by trial and error.

The "best-fit" surface is fitted to the data using the Matlab "griddata" function. Plots are produced using the "mesh" function. Surface normals can be generated for each square of the best-fit surface using the "surfnorm" function, and may be plotted using the "quiver3" command. Once surface normal information is available the angles of the crack face can be quantified with position within the rail, e.g. with depth, or with transverse position across the rail head.

4.4.2 Illustration of use

To illustrate the use of the model, simulated data were generated for a simple simulated inclined crack (Figure 18). Both upturning and downturning cracks were simulated (Figures 19 and 20) to illustrate the appearance of the crack and surface normals in each case.

For a real crack data were selected from the Hatfield crack visualisation model. A single crack was selected from those present between 78 and 96mm along the rail (the 'x' axis using the scale shown in Figure 21). Examples of output from the model are shown in Figures 22 and 23 for two different levels of smoothing.

4.4.3 Application

The three-dimensional approach to analysis of the crack morphology data allows the shape of cracks to be easily visualised. If the surface orientation of each facet of the smoothed representation of the crack were tabulated, the method also offers the ability to quantify the changes in orientation of the crack face with depth and position within the rail. If greater data reduction is required, for example to examine crack inclination angle on a given plane, a plane may be taken through the smoothed data and these angles found. This would offer the same data reduction capability provided by the two-dimensional approach to examination of the cracks, but with the advantage of smoothing the data, and allowing angles to be found independently of the position of the original data points.

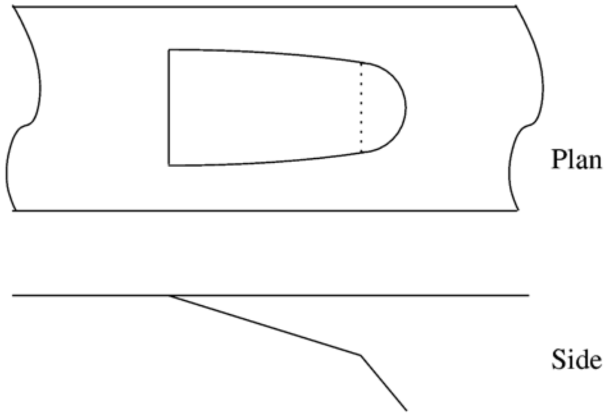

Figure 18 Plan and side views of the downturning crack generated to illustrate the output of the Matlab based model. The rail runs from left to right.

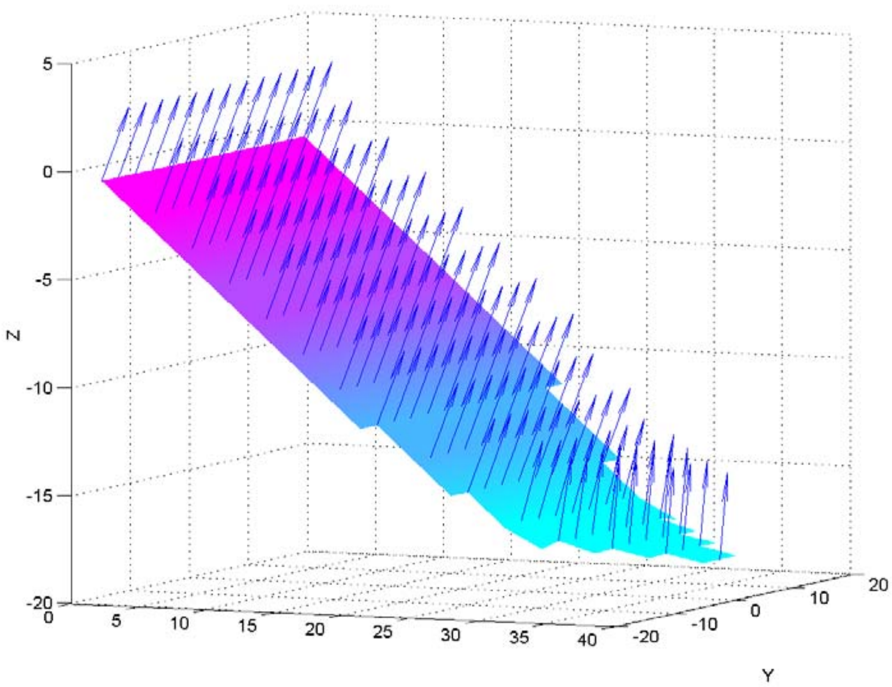

Figure 19 Output from the Matlab model for an upturning crack. Arrows represent normals to the surface of the crack. 'z' represents increasing depth into the rail, 'y' is the transverse direction across the rail.

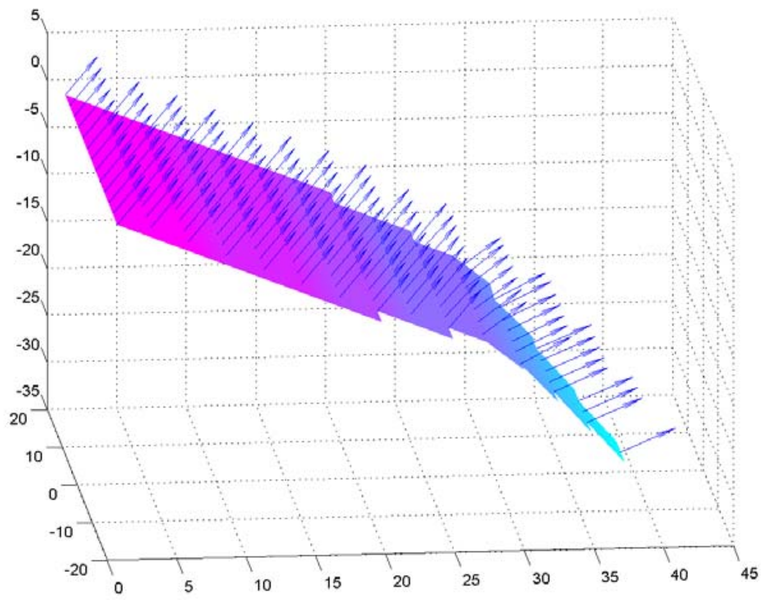

Figure 20 Output from the Matlab model for a downturning crack. Arrows represent normals to the surface of the crack.

Figure 21 shows a "transparent" view of the cracked rail, with lines showing the position of the crack surfaces inside the rail head. A smoothed surface was fitted to a small selection of these crack surfaces using the Matlab routine described above, with two different levels of smoothing applied. Figure 22 shows the output of the model with light smoothing, and Figure 23 with heavy smoothing. In these figures "Y" is position across the rail head, "Z" is depth below the rail surface, and the cracks lie inclined in the longitudinal direction of the rail.

In both Figures 22 and 23 the surface of the crack is shown using solid colour, made up of a series of facets generated from adjacent points fitted to the crack surface data. Each facet has the direction normal to its surface indicated by a thin arrow. Where these arrows like parallel to one another (close to the surface, z=0, in this case) they show that the crack lies approximately on a plane within the rail head. Where the arrows cross, this indicates that the facets lie in different planes, and that the crack is of a more complex shape. In the current case, the deepest parts of the cracks are forming a shallow "cup" or "ladle" shape at their deepest points. Heavier smoothing tends to bring out the underlying shape of the crack by removing local variations or roughness in its shape.

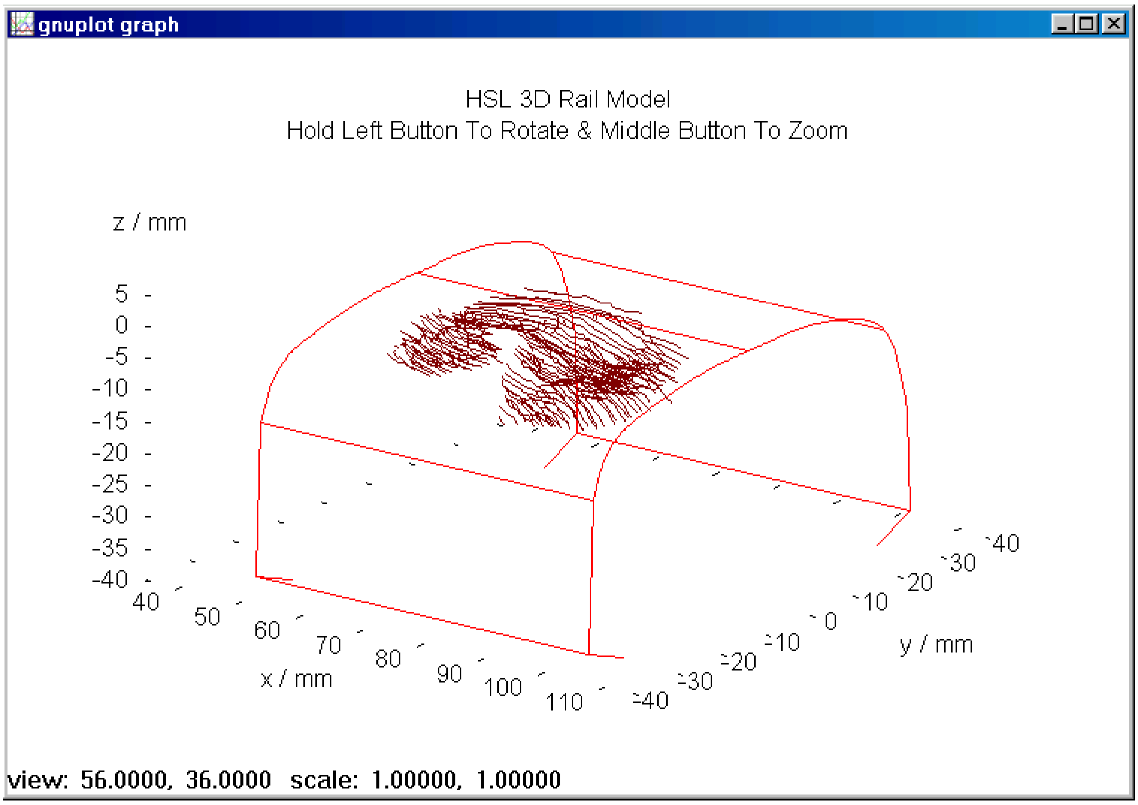

Figure 21 Data for a real crack was taken from the Hatfield crack visualisation model at positions between 78 and 96mm along the rail on the 'x' axis.

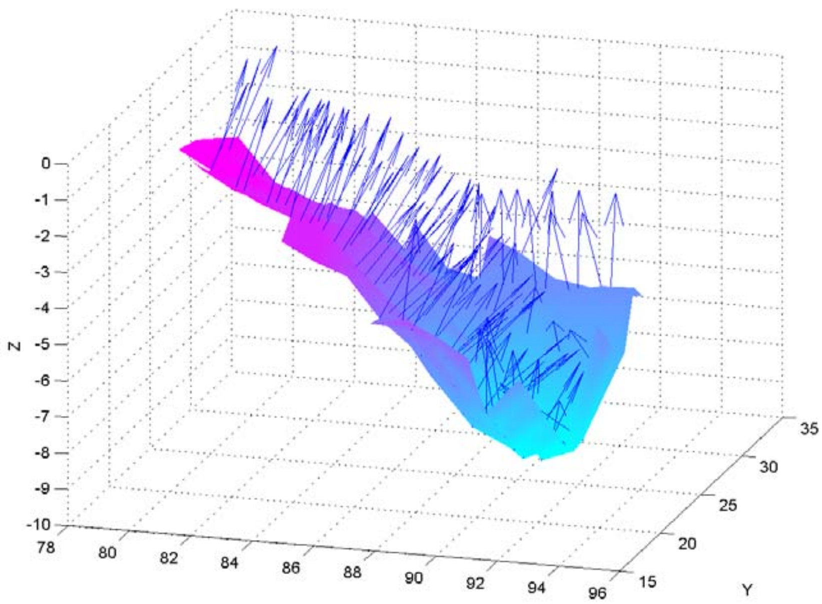

Figure 22 Output of the Matlab model for a real crack, using light smoothing. The upper part of the crack is similar to the simulated crack (Figures 18 and 19) with a uniform incline below the rail surface which lies at 'z' = 0. The lower part of the crack is much more complex than that of the simulated cracks.

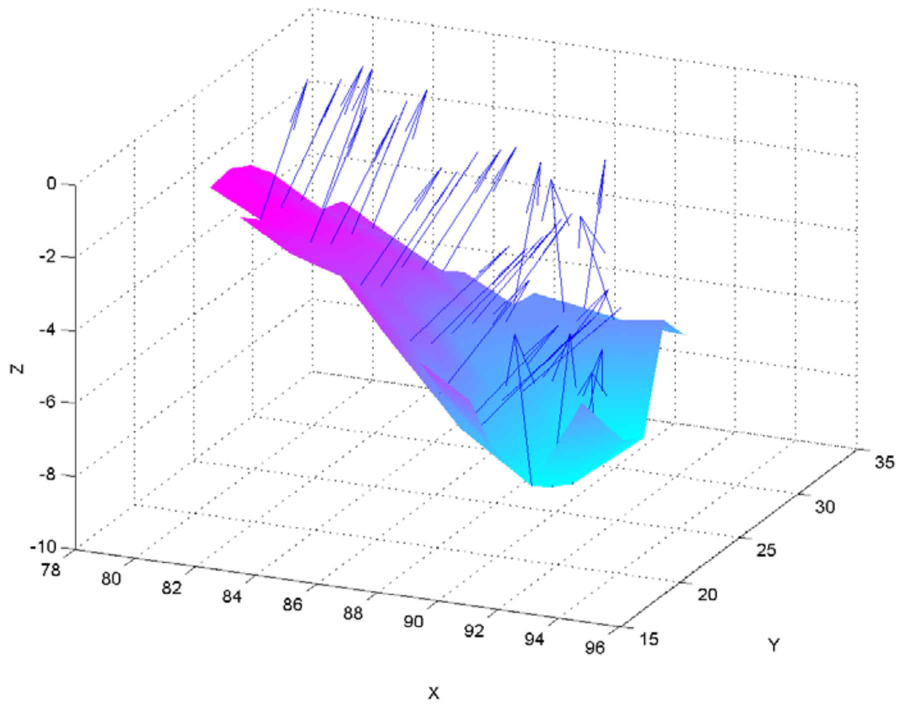

Figure 23 The same crack as shown in Figure 22, but with heavier smoothing of the incoming data.

5 CONCLUSIONS

The grinding of the rail section revealed a large number of cracks of various depths. Analysis of the data obtained from this exercise has enabled the following conclusions to be drawn:

1. Cracks grow at shallow angles, generally between 0° and 15°, until they reach a depth of approximately 6 mm.

2. The angle of cracks is particularly shallow between depths of 1.5 mm and 3 mm, with average angles of less than 1.5°.

3. The cracks tend to turn down into the rail head steeply at depths of over 6 mm. The majority of crack segments with depths above 7 mm have angles of over 30°.

4. Of the sample of cracks that were analysed for the relationship between surface length and depth, four lay outside the region expected by the Railtrack model. Therefore, these cracks were deeper than the Railtrack model predicted, based on the measured surface length of the cracks.

5. A three-dimensional model has been generated to help to visualise the cracks in the rail head.

References

[1] Railtrack plc. Rolling contact fatigue in rails: A guide to current understanding and practice. Technical report, Railtrack plc, 2001.

APPENDIX 1 UNIVERSITY OF SHEFFIELD REPORT ON VISUALISTION OF CRACKS

University of Sheffield
Project JR 31.086
Post Hatfield rolling contact fatigue
Additional work - visualisation of cracks

T Lim DI Fletcher A Kapoor

September 2, 2003

Contents

1 Executive Summary

A 3D model of a rail was developed using plotting software - Gnuplot v3.8j, which provides with an interactive capability for viewing the rail with internal cracks. The computer-based model closely represents the actual rail sample, which was taken from the Hatfield accident site. Model details:

- The model runs from a CD, with no software installation required
- The model is designed for use with Internet Explorer on Windows
- A three button mouse or wheel mouse is required to control the model
- Pre-selected views, interactive views, and cut-aways of the rail are available
- Selected views can be copied into other applications via the Windows clipboard
- Full code of the model is provided to allow for future changes or enhancements.

Following the development of the model, further study was carried out to establish a correlation between visible surface crack length and crack depth in the rail. A close agreement was found between the results for the Hatfield site and those in the literature. Generally, visible surface crack lengths of greater than 20 mm correspond to a crack depth of more than about 5 mm, whereas surface cracks of less than 20 mm gave a crack depth of less than about 5 mm.

2 Introduction

The Hatfield derailment investigation showed the primary cause of the accident was the fracture of the high rail as a result of rolling contact fatigue (RCF). To investigate this accident, the HSL project JR 31.086 has produced detailed data on the internal crack paths for a 300mm length of rail from the Hatfield site. These data were plotted using plotting software, Gnuplot v3.8j - to create a 3D rail model including the cracks. The package allows for 3D interactive viewing, and for cut-away section to be viewed. Correlation between the surface crack lengths and the crack depths were also investigated using the 3D model in combination with exterior photograph of the rail. Such correlations may be useful when inspecting rails that exhibit RCF cracks.

The main objectives are summarised as follows:

- To provide a simple means of visualising the internal crack data generated at HSL for the Hatfield rail.
- To correlate visible surface length of cracks with their internal dimensions

3 Terminology

Figures 1 and 2 illustrate the terminology used to describe the cracks.

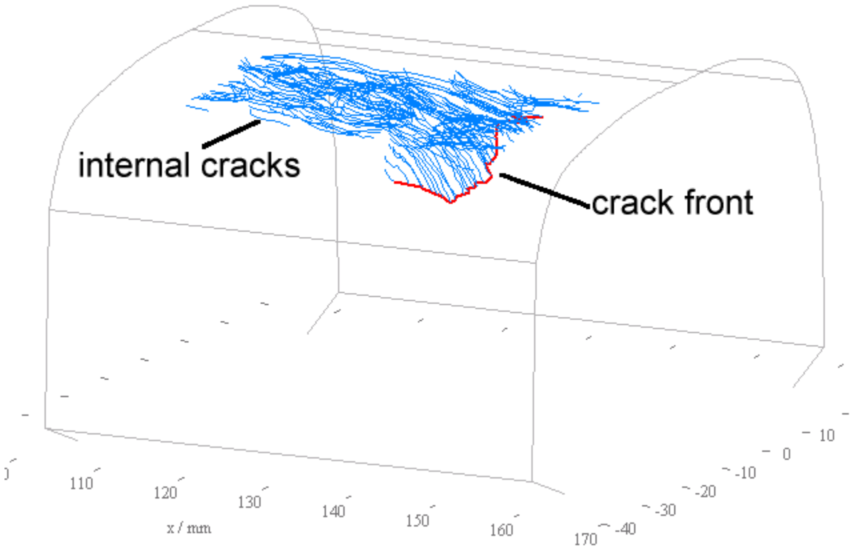

Figure 1: Graphical illustration of crack front and internal cracks

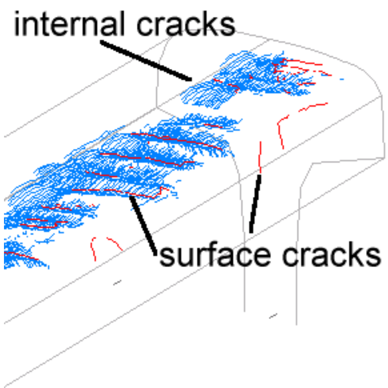

Figure 2: Graphical illustration of surface and internal cracks

4 Development of the 3D Rail Model

Data on the internal cracks in the Hatfield rail was available as digitised points in spreadsheet files, together with the original photographs of sections of the rail. These data were brought together to form a single data set with all crack positions specified relative to a single datum point. To visualise the exterior of the rail, its profile was approximated by linear functions at the rail base and polynomial functions at the curved railhead. The command-based plotting software used was Gnuplot v3.8j. A Windows based version was chosen for this project, but it is also available for Unix and Mac operating systems. The viewing software can be executed directly from the CD without any installation to the computer, allowing easy access to the model. The developed model is in 3D interactive format containing various crack views. This allows the view of the rail and cracks to be generated from all angles, and includes cut-away sections that can reveal the internal position of cracks. Static views of the model can be generated via the Windows Clipboard and pasted into other applications as required.

For ease of presenting the computer-based rail model, viewing pages were set up using HyperText Markup Language, HTML. This may be viewed using an Internet browser such as Internet Explorer. The execution of the plotting files is tied up with the HTML code by means of batch files (.bat). These batch files are executed by Windows, which is programmed to launch the appropriate files to view the 3D rail model by selecting a button displayed in the browser. Having developed this, various viewing options have been preset to view the 3D rail model. Amongst them are full and close-up views of internal cracks, surface cracks, crack fronts, cut-away sections of the rail, and various combinations. Additional viewing set-ups are possible by editing the command-file that Gnuplot reads from, although this is highly unlikely to be required.

5 Important Points in the Development of the Rail Model

- Minor modifications made to the supplied crack data - During the development of the Gnuplot model, the digitised data supplied by the HSL was continually checked with the original digital photographs - also supplied by HSL. Where differences were found between the data and the photographs, corrections were made so that the final dataset agreed with the photographs. These minor modifications are detailed in Appendix A.1. Overall resolution was limited to the cracks revealed by Magnetic Particle Identification, MPI which reveals all but the very finest of cracks.

- Rail profile data of the rail sample - The rail profile for the Hatfield railhead was available, and is represented by polynomial equations in the model. The rail web and foot profile were not available and within the model, these regions were made based on the profile of another specimen of rail. Since the cracks of interest are in the railhead, this approximation has no effect on the accuracy of the model.

- Hardware requirement for viewing - Viewing the 3D model interactively in the Gnuplot graphics window using "mouse-control" requires a "three-button mouse". The model is designed for viewing using Internet Explorer on Windows. It has been tested on Windows 2000, XP and ME. Memory requirements are low, but for the best performance when using the interactive views a fast video card is important.

6 Gnuplot v3.8j (Advanced users only - for simple interface see Section 7)

Gnuplot is a command line driven program for producing 2D and 3D plots. The Gnuplot command-file can be written using any text editor, such as Windows Notepad. The command-file contains instructions for Gnuplot to generate a plot. Table 1 highlights some of the important commands in the command-file that were used to create the 3D model.

Command	Description
#	Ignore entire line
,	Defines a continuation onto the next line
set title	Sets the main title of the plot
set view	Sets the view of plotting the model
set noborder	Removes the borders of the plot
set xrange	Defines the range of values of the x-axis
set yrange	Defines the range of values of the y-axis
set zrange	Defines the range of values of the z-axis
splot	Command to plot a 3D graph
index	Selects sets of entities in the data file (in this case, entities are lines) to be plotted
using	Determines how the columns in the data-file are to be interpreted

Table 1: Important Gnuplot commands used in the command file. Further details are available in the Gnuplot manual [1]

By manipulating the x, y and z range values, cut-away and close-up views can be produced (see appendix A2 and A3). If altering the pre-written plot file, care should be taken in defining the z-range values to ensure a correct aspect ratio of the model. Adjustment can be made using the mouse button as explained in the following section, however settings are only kept during the current Gnuplot run.

6.1 Executing the 3D Rail Model

The Gnuplot command window must be launched first (by double clicking on wgnuplot.exe) to be able to view the 3D model of the rail. After launching Gnuplot select the Open button and change the types of files to be read to All Files (*.*) at the Files of types scroll option (see Figure 3). Finally, locate the Gnuplot command file (e.g. adj_10.txt, full_2.txt, rail_2.txt and zoom2.txt) in the appropriate folder to launch the interactive graphics window displaying the plotted 3D rail model (see Figure 4).

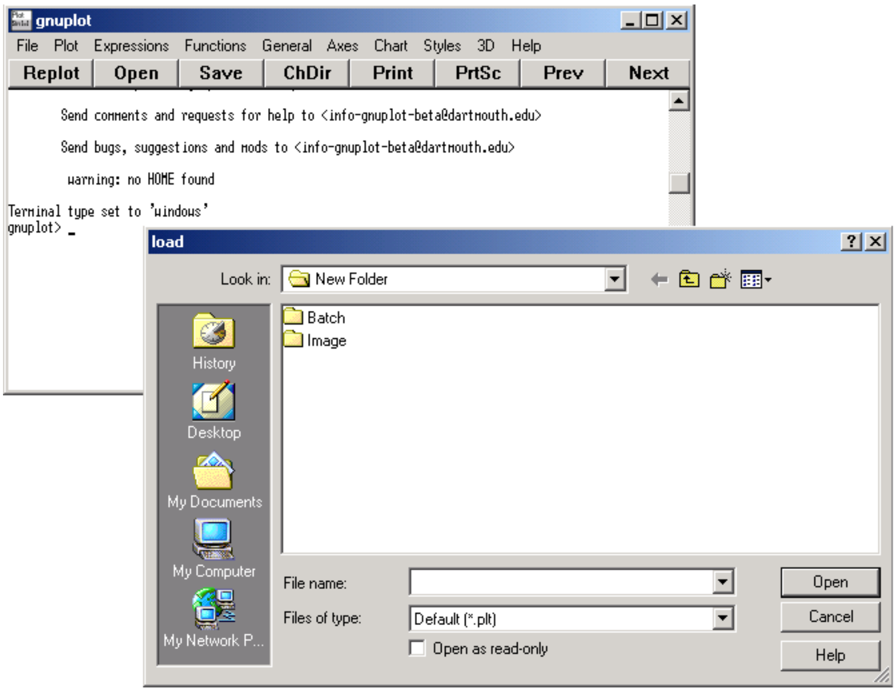

Figure 3: Opening the command file in Gnuplot

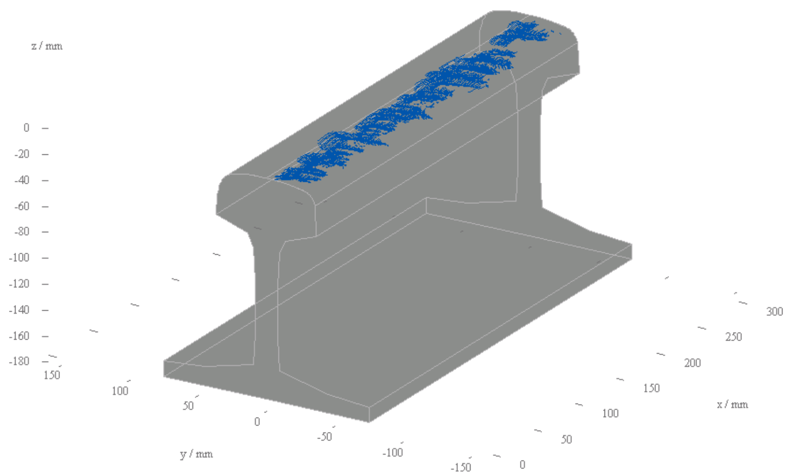

Figure 4: Viewing window of a 3D rail model

6.2 Viewing the model using Gnuplot

The 3D rail model appears in a window separate from the Gnuplot command window. Interactive viewing is enabled using the mouse or keyboard. Tables 2 and 3 give a list of the controls to view the model for both mouse and keyboard option.

Command	Description
left-click	Hold to rotate the model
wheel	Hold and drag side-to-side to control zoom (left = zoom out; right = zoom in). Hold and drag up-and-down to control z-axis scale (up = increase; down = decrease)
ctrl+shift+ wheel	Hold to offset x-y plane (move mouse up and down)

Table 2: Control of interactive Gnuplot window using the mouse. The use of a wheel or three button mouse is required.

Command	Description
arrow-keypad	To rotate
H	Help Commands - More Keyboard Commands can be seen in Gnuplot command window. Execution of these commands can only be carried when the interactive viewing window is selected

Table 3: Control of interactive Gnuplot window using the keyboard.

Centralising the area of interest at certain views for "zooming" cannot be done in the graphics window but can be achieved by editing the command-file to define the appropriate axis ranges. The angle of rotation about the x and y-axis is restricted to only 180 degrees, whereas the angle of rotation about the z- axis is not.

7 Viewing through Internet Explorer

The 3D model has been preset at various viewing angles with different combination of cracks, i.e. surface cracks, internal cracks and crack fronts. These views may be seen by launching the HTML file - "cover.html". By selecting the appropriate drive to read the files from (CD may be inserted in drive D, E or F depending on the computer settings), various preset views of the rail model with cracks can then be seen (see examples in Figures 5, 6 and 7). Interactive views of the models will appear when the corresponding option button is selected. Before the plot windows opens a Windows security check window may appear on screen. Choose the "Open" button to run the program from the CD. The following combinations of preset views are made available:

- Rail model with internal cracks

- Rail model with internal cracks and crack fronts
- Rail model with internal cracks and surface cracks
- Rail model with internal cracks, surface cracks and crack fronts
- Rail model with surface cracks
- Rail model with crack fronts
- Rail model with surface cracks and crack fronts
- Overview of internal cracks
- Segment view of cracks: 0-28, 28-60, 60-95, 95-112, 112-150, 150-185, 185-215,219-250, 250-310 mm from the end of the rail sample.

Colour and line settings in the graphics window are set to the Gnuplot default unless Wgnuplot.ini file is exported from the compact disk into the primary hard drive under Windows folder. To close the plot window, select the OK button on the pop-up box, which floats in front of the graph. Otherwise, move the box aside to continue viewing the plot. This software has been tested on Windows 2000, XP and ME.

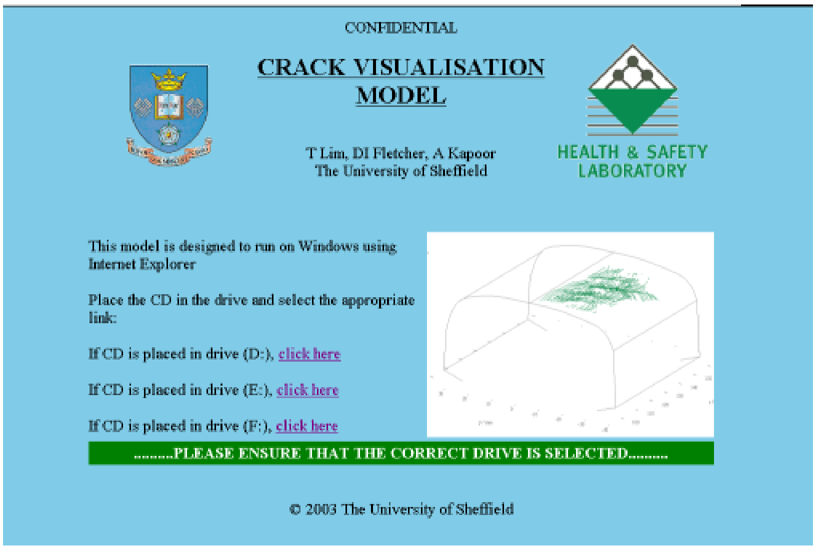

Figure 5: Cover page - selection of correct disk drive to read files from

8 Additional interactive capabilities

By clicking on the top-left icon on the interactive viewing window, a scroll down list will appear providing more interactive commands to choose from (see Figure 8). Apart from the standard windows menu, two additional items are available, Options and About. The later provides information about the software. Options gives a lists of choices to edit the appearance on the Gnuplot plotting window. Table 4 summarises the items in the Options menu.

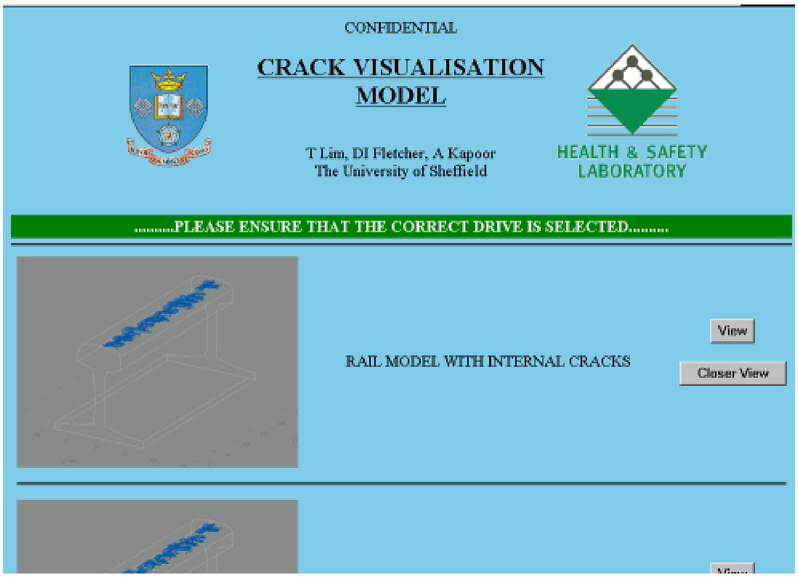

Figure 6: First page - viewing page of various crack views

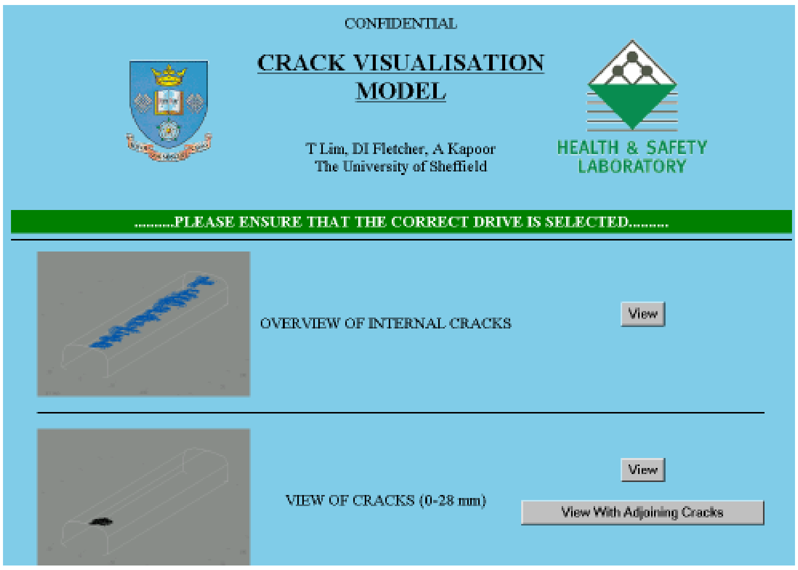

Figure 7: Second page - viewing page of individual segments of cracks

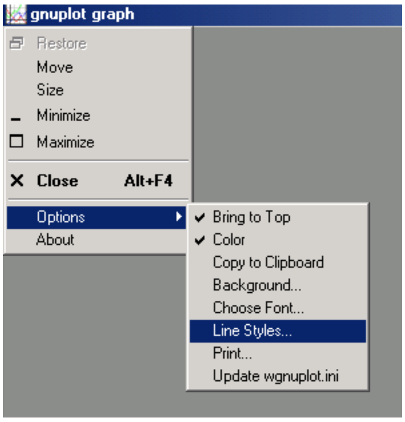

Figure 8: Scroll menu providing with additional interactive features to the plot

Command	Description
Bring to Top	Brings graph to the top after opening the command-file
Color	Sets the colour settings of lines to either prescribed colours or monochrome
Copy to Clipboard	Copies a bitmap and a Metafile picture for insertion into other applications
Background...	Sets the viewing window background colour
Choose Font...	Selects the font used in the graphics window
Line Styles...	Allows customisation of the line colours and styles. Lines are numbered in sequential order as appears in the data file "plotting" line in the command-file.
Print...	Prints the graphics window
Update wgnuplot.ini	Saves the changes made to the appearance of the plot to file. Wgnuplot.ini file is only read if it is saved in the primary hard drive under the WINDOWS folder

Table 4: Description of the options available in the Gnuplot graphics window. Further details are available in the Gnuplot manual [1]

9 Results and Discussion

9.1 Visualisation of 3D Rail Model

Figures 9, 10 and 11 present some of the views of the rail and cracks obtained from the model (these views are best seen in the electronic copy of this report, as they do not print well).

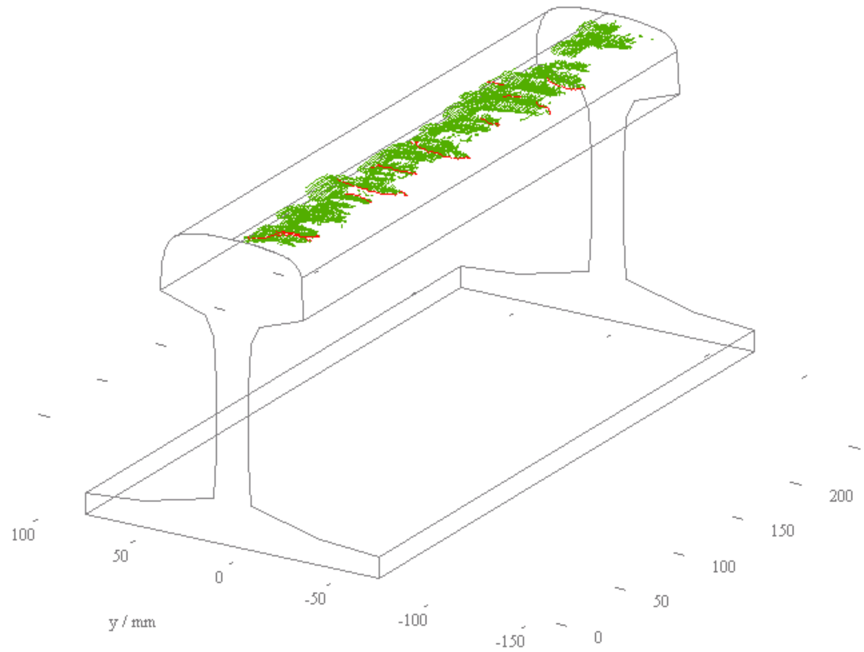

Figure 9: 3D plot of the rail model showing internal cracks and crack fronts

9.2 Correlation of visible surface crack length with crack depth

To investigate the correlation between visible surface crack length and crack depth, the measured characteristics were defined as shown in Figure 12. Straight lines were used to measure distances, rather than following the intricate path of each crack. The computer-based model of the rail with cracks was used to establish the internal crack length and depth. The distance between the ends of the crack mouth on the surface of the rail was calculated using image-processing software, working with the original photographs of the rail, prior to the sectioning used to reveal the internal cracks. For length and depth correlations the longest and deepest cracks respectively were found (22 cracks in each case). Because of the branching present in many cracks, the longest and deepest sets of cracks did not contain the same cracks, so although surface crack lengths are similar for the longest and deepest results, it is not necessarily the same cracks which were being measured. Table 5 and 6 shows the results obtained.

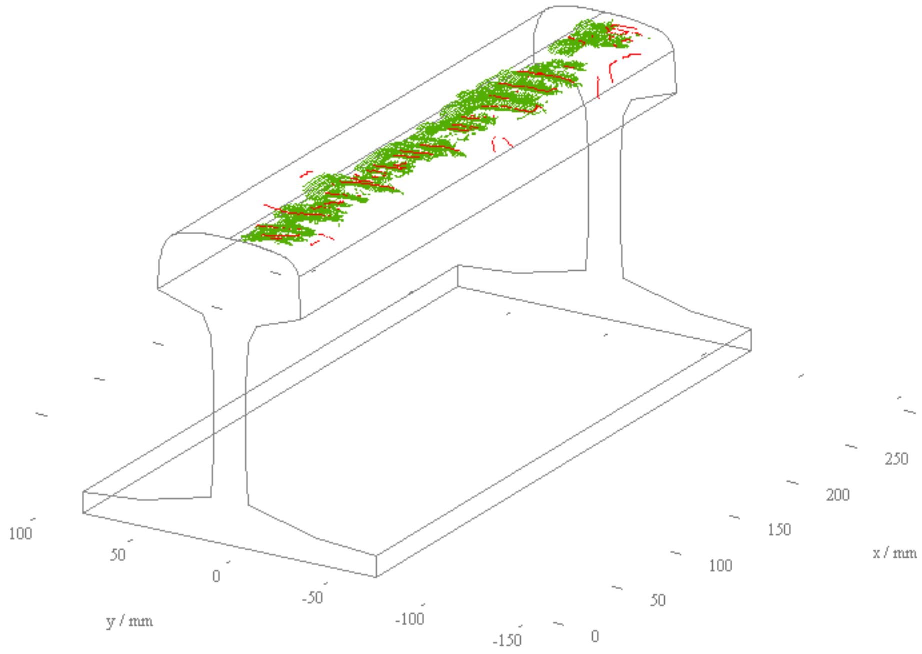

Figure 10: 3D rail model showing internal and surface cracks

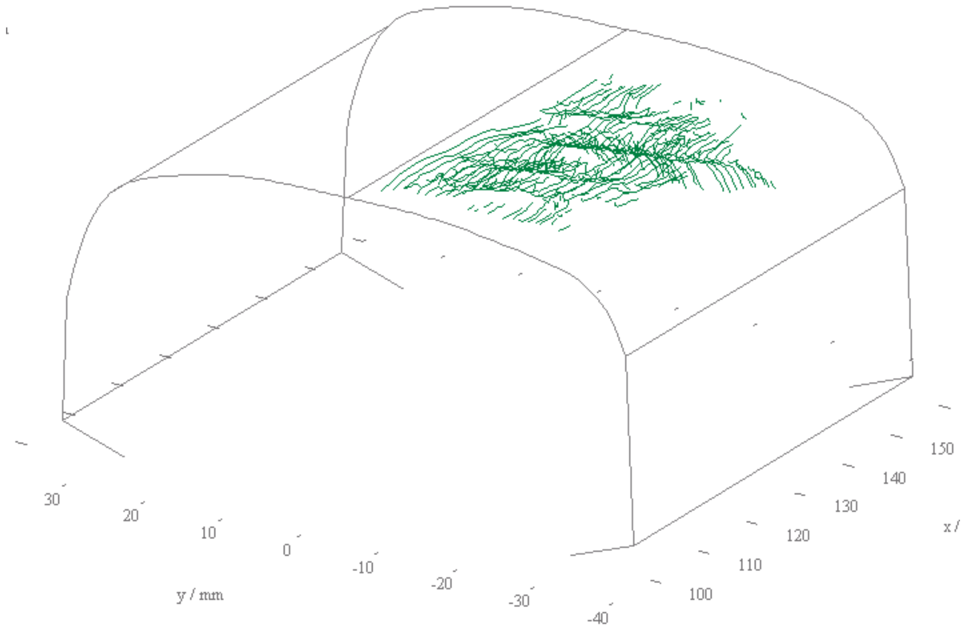

Figure 11: Close-up view of a segment of internal cracks along the length of the rail

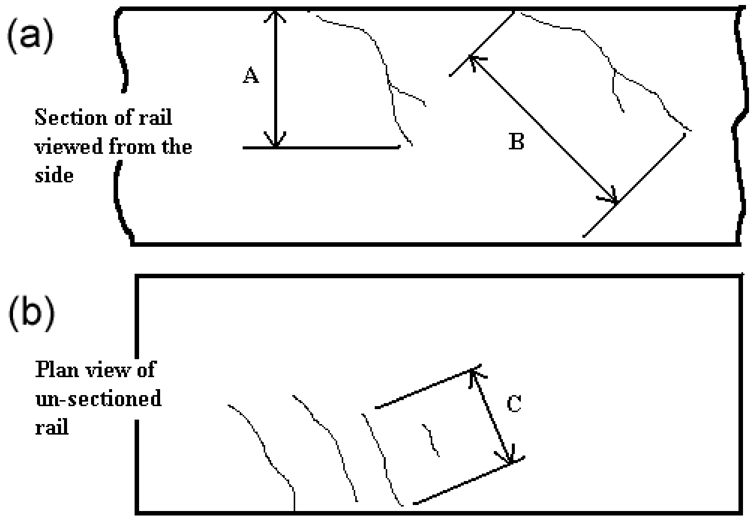

Figure 12: Definitions of crack measurement. (a) A section view of the rail. Crack A is deeper than crack B, although crack B is longer, hence different groups of cracks were identified when searching for the longest and deepest sets. (b) Plan view of the rail prior to sectioning, illustrating visible crack lengths.

Crack	Surface crack length (mm)	Crack Depth (mm)
1	5.33	4.02
2	17.53	6.22
3	34.82	7.80
4	31.36	6.53
5	12.54	6.33
6	9.99	3.88
7	10.59	5.00
8	24.46	10.71
9	10.71	3.37
10	8.98	3.10
11	13.18	5.80
12	12.00	3.06
13	14.73	4.80
14	17.67	10.00
15	9.39	3.16
16	11.81	5.00
17	8.60	4.69
18	25.94	6.32
19	9.28	6.20
20	25.97	6.63
21	25.89	9.80
22	4.70	4.49

Table 5: Results of surface crack length and crack depth obtained form the model

Crack	Surface crack length mm	Internal crack length mm	Crack angle deg
1	17.47	15.32	12.43
2	34.82	17.24	30.75
3	31.56	16.81	14.07
4	12.67	12.89	19.70
5	9.86	13.26	15.29
6	15.33	14.77	18.94
7	23.88	21.42	33.24
8	9.84	15.06	22.79
9	10.30	11.04	14.30
10	8.80	9.74	13.44
11	12.06	17.37	9.38
12	11.69	9.12	17.66
13	15.30	13.69	21.47
14	17.37	17.19	44.40
15	9.01	9.93	20.17
16	11.16	15.56	15.30
17	8.68	15.07	12.69
18	25.93	16.97	11.19
19	9.14	17.32	14.16
20	25.98	24.23	11.98
21	25.50	14.31	55.17
22	5.51	14.49	19.64

Table 6: Results of surface crack length and internal crack length obtained form the model

Figure 13 and 14 allows the relationship between internal and external (i.e. visible) crack lengths to be investigated. It may initially appear that the plotted points are scattered around a straight line. However, information from Railtrack suggests that a different type of relationship, as shown in Figure 15, is to be expected [2]. Figure 16 shows the same plot with superimposed data from the Hatfield rail.

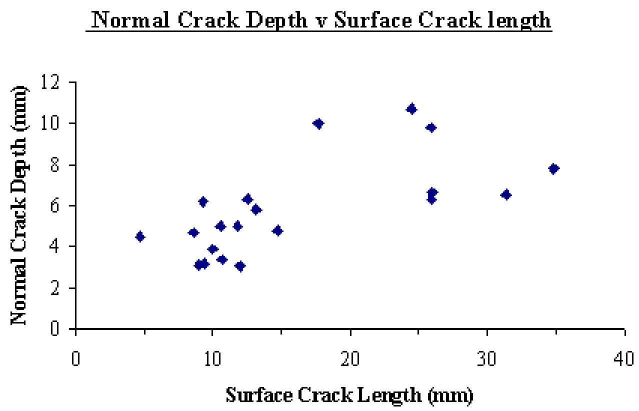

Figure 13: Graph of internal crack depth vs. visible surface crack length (taken from Table 5)

It can be seen that there is a general agreement between the current results and the Railtrack literature. This indicates that the crack growth pattern in the rail sample is consistent with the results previously obtained by Railtrack. However, some points do lie outside the shaded region in Figure 16. The rail sectioning and data collection has been estimated to produce a maximum error (particularly cracks approaching gauge face) of 1 mm, but even if this is taken into consideration some points would remain outside the shaded region, and many others would still remain close to its borders.

It is known that the Hatfield rail was ground. Grinding will remove the material from the top of the rail, and from the gauge face. This would alter the crack length and depth, but the exact amount of material removed from the rail section considered here is not know to the authors. For typical grinding operations the removed thickness is less than a millimeter, and so the changes in crack length and depth will be of this order.

10 Subsurface Cracks

Figures 17 and 18 indicate that the rail sample used to generate the 3D rail model contains subsurface cracks tending towards the centre of the railhead. Typically the visible surface crack at the rail gauge face is close to the subsurface boundary of the crack, while the crack continues sub-surface 10 - 15 mm towards the rail centre, beyond the visible surface crack. (As with other images taken from the model, Figure 17 is better viewed in the electronic version of this report, rather than in the printed version.)

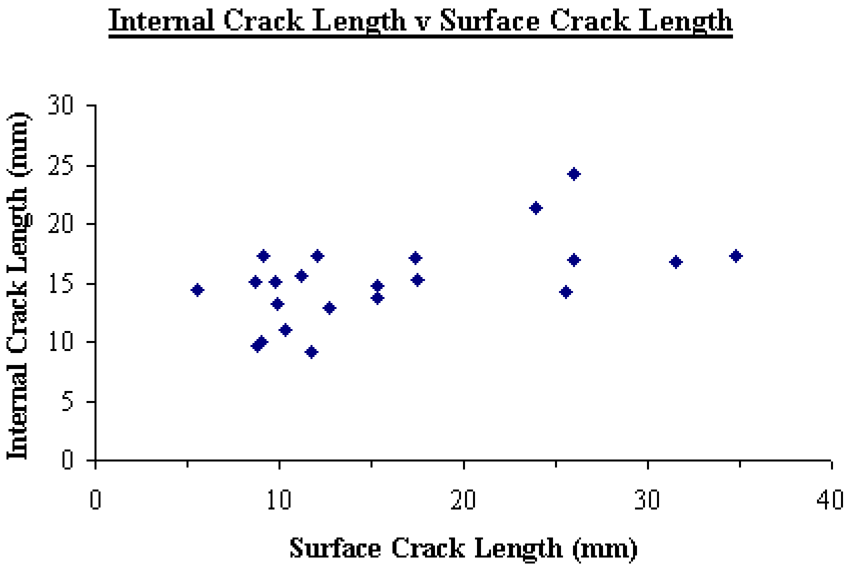

Figure 14: Graph of internal crack length vs. visible surface crack length (taken from Table 6)

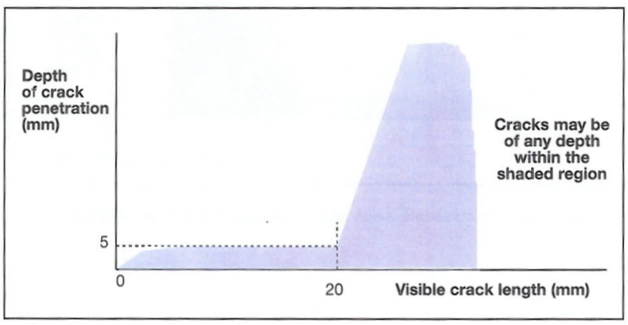

Figure 15: Relationship between depth of crack penetration and visible crack length [2]

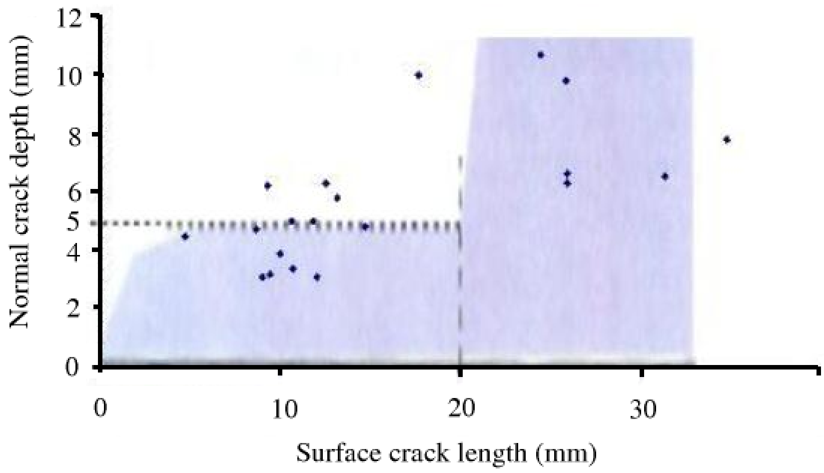

Figure 16: Combined plot of normal crack depth and surface crack length obtained from Railtrack and Hatfield rail

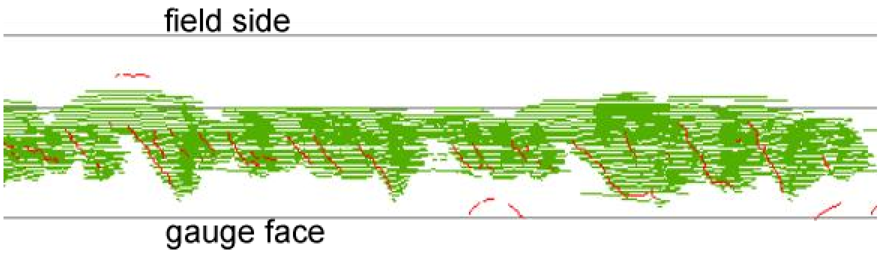

Figure 17: Plan view of the rail head from the 3D rail model, indicating existence of subsurface cracks. Visible crack mouths are shown by dark lines, light lines indicate internal cracks, which extend beyond the visibly cracked region toward the centre of the rail head.

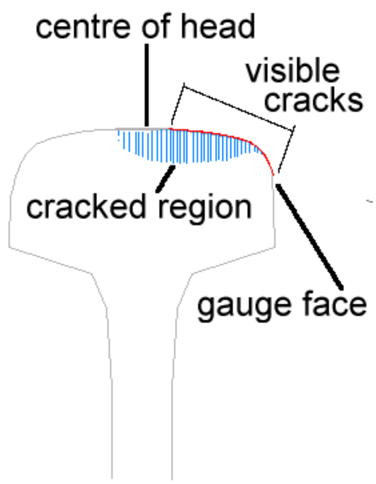

Figure 18: Side view of the rail head from the 3D rail model, indicating existence of subsurface cracks.

11 Conclusion

An interactive 3D model of a sample rail with cracks was developed using data from the Hatfield rail. The model can provide pre-selected views, interactive views, and cut-aways of the rail. Operation is possible through a web browser, but all the code required to modify the model in future is also supplied. The model was used to establish a correlation between the visible surface crack length and crack depth.

References

[1] *GNUPLOT - An Interactive Plotting Program, Version 3.8j.* http://www.gnuplot.info/, 2003.

[2] Railtrack plc. Rolling contact fatigue in rails: A guide to current understanding and practice. Technical report, Railtrack plc, 2001.

A Appendix

A.1 Modifications made to the original data to facilitate plotting

Where minor differences were identified between the tabulated data and the digital photographs of the sectioned rail supplied by HSL, changes were made to the data to ensure it agreed with the photographs. Figure A-1 illustrates this.

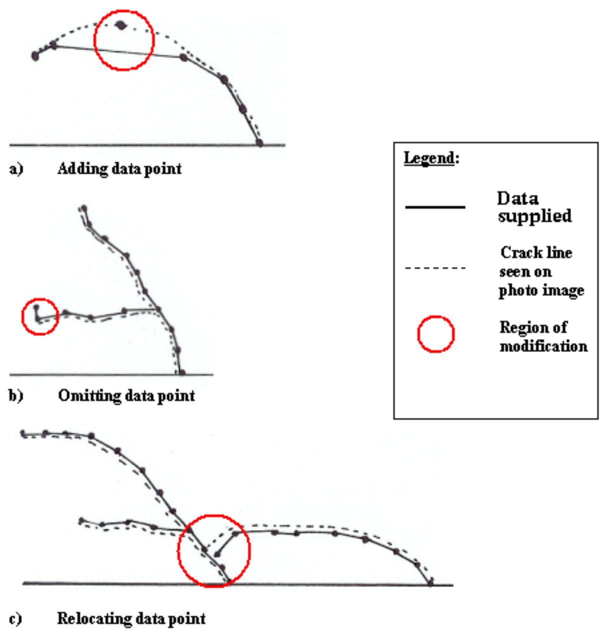

Figure A-1: Modifications made to the original data

A.2 Index of Crack Groups at Various Grind Depths

Plots of cracks at only a specific grind depth into the rail can be produced by restricting the range of data from the input file which is to be plotted. Data for the cracks are arranged in a series of blocks which have sequential index numbers from 0 to 1908. Table A-1 shows which data blocks correspond to which grind depths.

A.3 Index range of other crack groups

The data supplied with the model contains data blocks for crack fronts, crack mouths and the outer profile of the rail in addition to those for cracks which are tabulated in Table A-1. These additional data sets are stored in the files listed in Table A-2.

First data set	Last data set	Grind depth / mm
0	0	7.24
1	1	8.24
2	6	9.02
7	14	10.69
15	29	11.72
30	48	12.72
49	63	13.64
64	82	14.69
83	117	15.65
118	161	16.79
162	215	17.75
216	262	18.86
263	336	19.77
337	422	21.09
423	515	21.88
516	584	22.85
585	683	23.84
684	773	24.76
774	869	25.77
870	962	27.59
963	1055	28.58
1056	1165	29.52
1166	1253	30.43
1254	1342	31.30
1343	1431	32.24
1432	1528	33.35
1529	1631	34.59
1632	1723	35.95
1724	1782	37.21
1783	1821	38.42
1822	1853	39.68
1854	1873	40.76
1874	1887	41.82
1888	1899	43.49
1900	1906	45.00
1907	1908	46.34

Table A-1: Index of crack groups at various grind depths

Description	Filename	Number of blocks
Crack Front	crackfront.txt	11
Surface Crack	cracksurface.txt	96
Additional Rail Profile	inter.txt	3

Table A-2: Filenames for data on crack fronts, crack mouths and the outer rail profile.

A.4 Command file and data window

Figures A-2 and A-3 provide a record of the Gnuplot command file, and an example of the data file format.

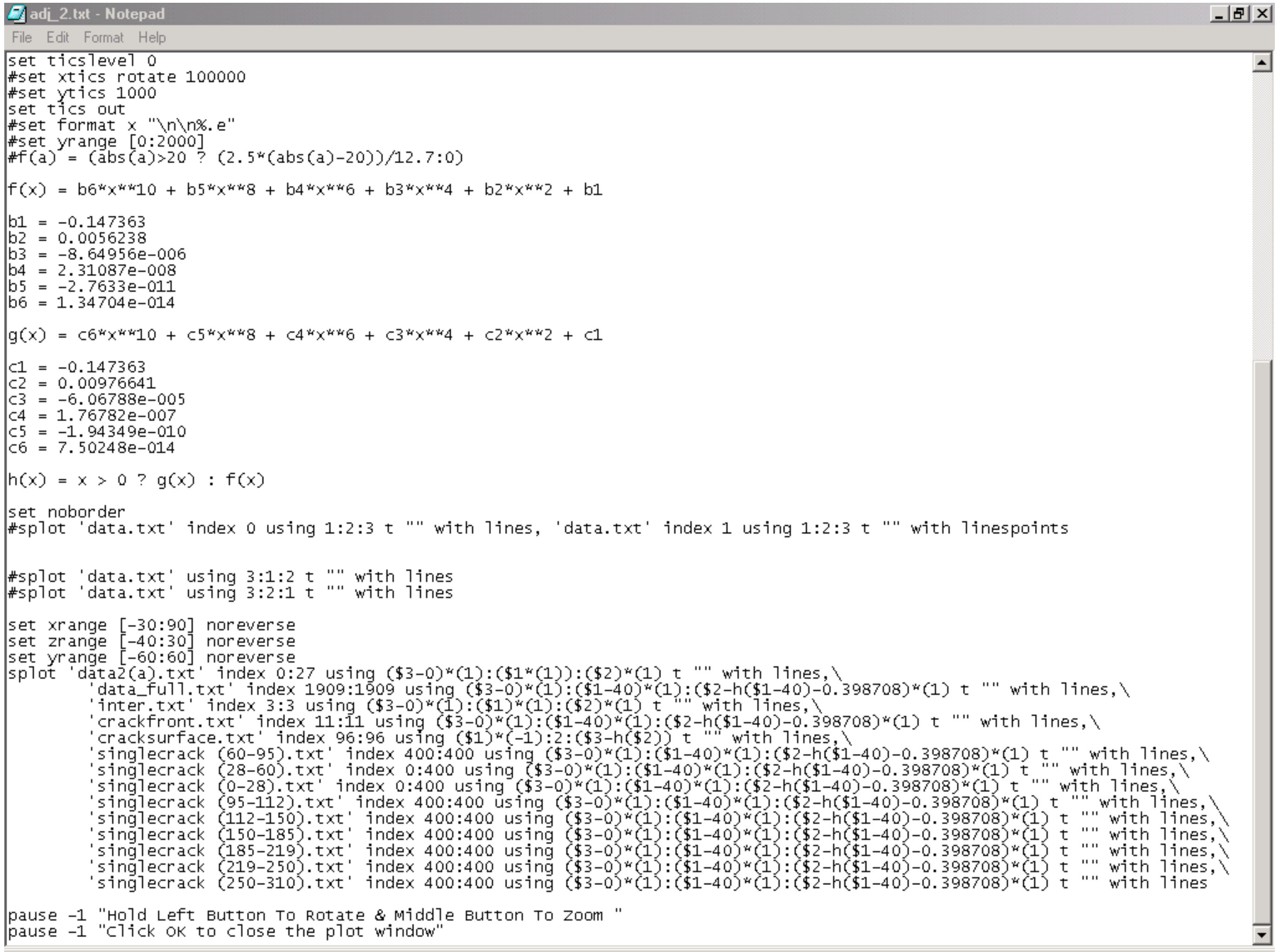

```
adj_2.txt - Notepad
File Edit Format Help
set ticslevel 0
#set xtics rotate 100000
#set ytics 1000
set tics out
#set format x "\n\n%.e"
#set yrange [0:2000]
#f(a) = (abs(a)>20 ? (2.5*(abs(a)-20))/12.7:0)

f(x) = b6*x**10 + b5*x**8 + b4*x**6 + b3*x**4 + b2*x**2 + b1

b1 = -0.147363
b2 = 0.0056238
b3 = -8.64956e-006
b4 = 2.31087e-008
b5 = -2.7633e-011
b6 = 1.34704e-014

g(x) = c6*x**10 + c5*x**8 + c4*x**6 + c3*x**4 + c2*x**2 + c1

c1 = -0.147363
c2 = 0.00976641
c3 = -6.06788e-005
c4 = 1.76782e-007
c5 = -1.94349e-010
c6 = 7.50248e-014

h(x) = x > 0 ? g(x) : f(x)

set noborder
#splot 'data.txt' index 0 using 1:2:3 t "" with lines, 'data.txt' index 1 using 1:2:3 t "" with linespoints


#splot 'data.txt' using 3:1:2 t "" with lines
#splot 'data.txt' using 3:2:1 t "" with lines

set xrange [-30:90] noreverse
set zrange [-40:30] noreverse
set yrange [-60:60] noreverse
splot 'data2(a).txt' index 0:27 using ($3-0)*(1):($1*(1)):($2)*(1) t "" with lines,\
        'data_full.txt' index 1909:1909 using ($3-0)*(1):($1-40)*(1):($2-h($1-40)-0.398708)*(1) t "" with lines,\
        'inter.txt' index 3:3 using ($3-0)*(1):($1)*(1):($2)*(1) t "" with lines,\
        'crackfront.txt' index 11:11 using ($3-0)*(1):($1-40)*(1):($2-h($1-40)-0.398708)*(1) t "" with lines,\
        'cracksurface.txt' index 96:96 using ($1)*(-1):2:($3-h($2)) t "" with lines,\
        'singlecrack (60-95).txt' index 400:400 using ($3-0)*(1):($1-40)*(1):($2-h($1-40)-0.398708)*(1) t "" with lines,\
        'singlecrack (28-60).txt' index 0:400 using ($3-0)*(1):($1-40)*(1):($2-h($1-40)-0.398708)*(1) t "" with lines,\
        'singlecrack (0-28).txt' index 0:400 using ($3-0)*(1):($1-40)*(1):($2-h($1-40)-0.398708)*(1) t "" with lines,\
        'singlecrack (95-112).txt' index 400:400 using ($3-0)*(1):($1-40)*(1):($2-h($1-40)-0.398708)*(1) t "" with lines,\
        'singlecrack (112-150).txt' index 400:400 using ($3-0)*(1):($1-40)*(1):($2-h($1-40)-0.398708)*(1) t "" with lines,\
        'singlecrack (150-185).txt' index 400:400 using ($3-0)*(1):($1-40)*(1):($2-h($1-40)-0.398708)*(1) t "" with lines,\
        'singlecrack (185-219).txt' index 400:400 using ($3-0)*(1):($1-40)*(1):($2-h($1-40)-0.398708)*(1) t "" with lines,\
        'singlecrack (219-250).txt' index 400:400 using ($3-0)*(1):($1-40)*(1):($2-h($1-40)-0.398708)*(1) t "" with lines,\
        'singlecrack (250-310).txt' index 400:400 using ($3-0)*(1):($1-40)*(1):($2-h($1-40)-0.398708)*(1) t "" with lines

pause -1 "Hold Left Button To Rotate & Middle Button To Zoom "
pause -1 "Click OK to close the plot window"
```

Figure A-2: Graphical example of command-file window

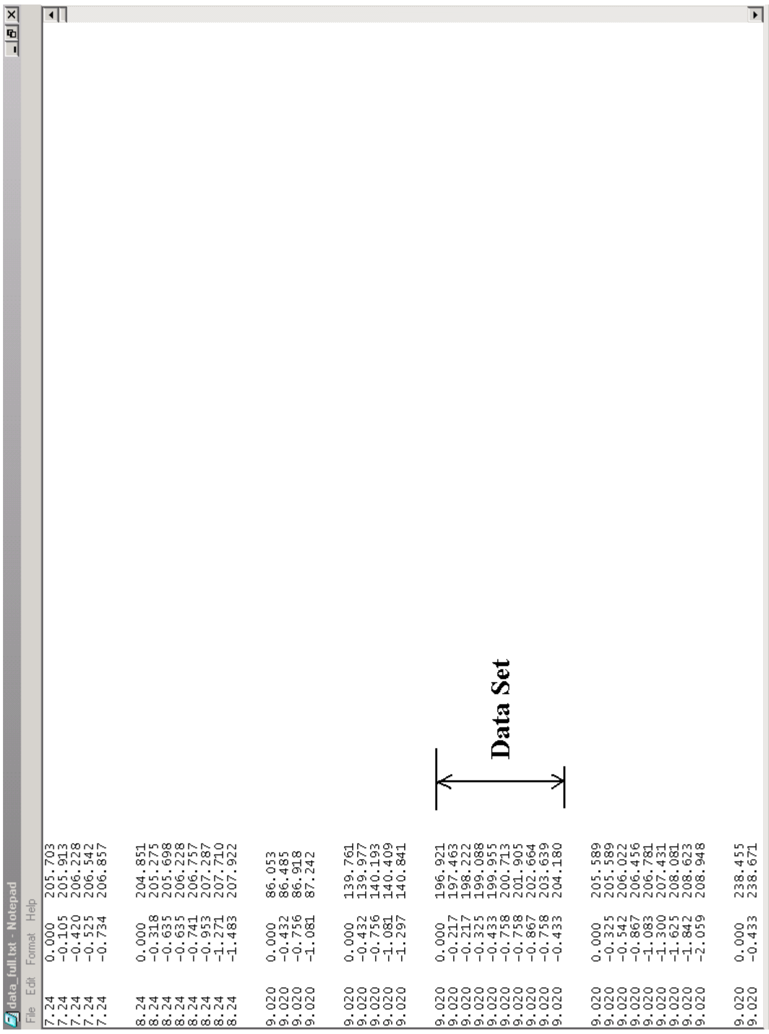

Figure A-3: Graphical example of data-file window